Highlights

Connectivity, conservation and catch: understanding the effects of dispersal between harvested and protected patches

Femke N. Reurik, Juan Segura, Frank M. Hilker

- We model metapopulations in which one of two patches is harvested.
- We found 5 (4) scenarios of how total population size (yield) respond to dispersal.
- Proportional harvesting shifts dynamics from source–source to effective source–sink.
- Increasing dispersal can lead to a rescue effect but may also lead to extinction.
- We establish when to keep patches isolated or to increase their connectivity.

Connectivity, conservation and catch: understanding the effects of dispersal between harvested and protected patches

Femke N. Reurik[a,*], Juan Segura[b], Frank M. Hilker[a]

[a]*Institute of Mathematics and Institute of Environmental Systems Research, Osnabrück University, Barbarastraße 12, Osnabrück, 49076, Germany*
[b]*Department of Finance and Management Control, EADA Business School, c/ Aragó 204, Barcelona, 08011, Spain*

Abstract

Overharvesting is a pressing global problem, and spatial management, such as protecting designated areas, is one proposed solution. This study examines how connectivity (in terms of dispersal rate) between protected and harvested areas affects the asymptotic total population size and the asymptotic yield, which are key questions for conservation management and the design of protected areas. We utilize a two-patch model with heterogeneous habitat qualities, symmetric dispersal and density-dependent growth functions in both discrete and continuous time. One patch is subject to proportional harvesting, while the other one is protected.

Our results show that increased dispersal does not always increase the asymptotic total population size or the asymptotic yield. Depending on the circumstances, dispersal enables the protected patch to rescue the harvested patch from overexploitation, potentially increasing both total population size and yield. However, high levels of dispersal can also lead to a lower total population size or even cause extinction of both patches if harvesting pressure is strong. The population in the protected patch needs to have high reproductive potential and the protected patch needs to be the effectively larger patch in order to benefit monotonically from increased dispersal. These findings provide a fundamental understanding of how dispersal influences dynamics in fragmented landscapes under harvesting pressure.

Keywords: symmetric dispersal, two-patch model, proportional harvesting, spatial management, source–sink dynamics, protected areas

*Corresponding author

Email addresses: femke.reurik@uni-osnabrueck.de (Femke N. Reurik), jsegura@eada.edu (Juan Segura), frank.hilker@uni-osnabrueck.de (Frank M. Hilker)

1. Introduction

Human activities are posing severe threats to wildlife species globally. For example, exploitation is recognised as the primary threat to species in marine ecosystems and the second greatest threat to those in terrestrial and freshwater ecosystems [1]. Another specific terrestrial example is the disruption of ungulate dispersal routes caused by human-made barriers, such as roads, railroads, pipelines and reservoirs. This disruption has led to significant declines in several species across Africa and Central Asia [2].

Establishing marine reserves and terrestrial protected areas is widely considered a viable strategy for preserving biodiversity effectively and sustainably. For instance, marine reserve models have been shown to increase fish biomass and mitigate the cumulative impacts of human activities such as harvesting in aquatic environments [3]. Furthermore, a recent meta-analysis indicates that fish biomass is, on average, 670% higher in marine reserves compared to unprotected areas [4]. The spillover effect from protected areas also boosts catches in adjacent harvested areas, as evidenced by data for the lobster *Palinurus elephas* in the Columbretes Islands marine reserve [5]. Similarly, terrestrial examples highlight the importance of protected areas. For example, hunting caused declines in the Garnet mountain lion population in Montana. After harvest closures, this population rebounded, enhancing emigration and metapopulation growth [6]. Additionally, there have been notable developments at the political level: the Convention on Biological Diversity established the "30 by 30 target" which aims to ensure that by 2030, at least 30% of terrestrial, inland water and marine and coastal areas are under effective restoration to enhance biodiversity [7].

Mathematical modelling is an indispensable tool in wildlife and ecosystem management, providing a structured method to explore how individual decisions impact broader ecological systems [8]. By investigating various scenarios, models can help identify unexpected outcomes that might hinder the achievement of conservation and management objectives.

Spatial harvesting models often focus on economic aspects, such as maximising yield or profit, when discussing the optimal harvesting policy [9, 10, 11, 12]. It is also well established that habitat heterogeneity [13, 14] and connectivity between habitats [15] are crucial factors to consider when aiming to protect biomass and biodiversity. Connectivity between habitats can be influenced by various measures, such as stepping stones and dispersal corridors, which can be modelled in mathematical frameworks through dispersal

variation. The role of dispersal has been examined in previous research, including a focus on age-structured dispersal patterns [16, 17] or dispersal distance [18].

However, the impact of dispersal strength and therefore connectivity remains unclear. Recent mathematical modelling has focused on the effects of increasing dispersal on the asymptotic total population size in two-patch models without harvesting [19, 20, 21, 22], showing that dispersal can be beneficial or detrimental, depending on its strength. Furthermore, experimental results on the impact of increased dispersal on the total population size confirm these modelling results: some studies report positive effects (e.g., yeast-like fungus *Aureobasidium pullulans* [23], budding yeast *Saccharomyces cerevisiae* [24]), while others report initially positive then negative effects (e.g., *Escherichia coli* [25]) or insignificant effects (e.g., *Drosophila melanogaster* [26]).

This leads to our research question: How do total population size and yield respond to increasing connectivity in a two-patch framework, where one patch is protected and the other one is harvested? We show that there are a total of five qualitative response scenarios of the asymptotic total population size to increasing dispersal. Additionally, the asymptotic yield responds with three different qualitative behaviours to increasing dispersal. We investigate how these responses are influenced by the heterogeneity of the patches, examining whether larger or smaller, and faster- or slower-growing protected patches yield different outcomes. Increasing harvest pressure alters the conditions for these responses to increased dispersal. Proportional harvesting results in the harvested patch being effectively smaller (reduced effective capacity) and exhibiting lower productivity (reduced effective growth rate). Overharvesting can cause a patch, when considered in isolation, to become non-persistent, turning it into a sink. Thus, when the larger patch is harvested, it becomes effectively the smaller patch, and with more intense harvesting, the initially larger patch transforms into an effective sink patch. Correspondingly, initial source–source dynamics in the absence of harvesting transforms into effective source–sink dynamics in the presence of sufficiently strong harvesting. Additionally, we interpret how increasing harvest pressure changes the parameter domains of the qualitatively different responses of the total population size and the yield to increasing dispersal.

2. Methods

In this Section, model equations for a two-patch model with density-dependent growth and proportional harvesting in both discrete and continuous time are presented. Secondly, we introduce effective parameters derived from proportional harvesting in a single population.

2.1. Model equations

The general structure of the system is described in Fig. 1. We consider two subpopulation sizes denoted N_{A} and N_{B}, which are linked by symmetric dispersal, which means that the dispersal intensity is identical in both directions. Each subpopulation follows an associated growth function characterised by intrinsic growth and carrying capacity (or intraspecific competition) parameters, exhibiting negative density dependence. Specifically, continuous-time logistic growth and its discrete-time counterpart, Beverton-Holt dynamics, are utilised. Additionally, one subpopulation is subject to proportional harvesting. Without loss of generality, we choose patch A to be the harvested patch and patch B to be the protected patch.

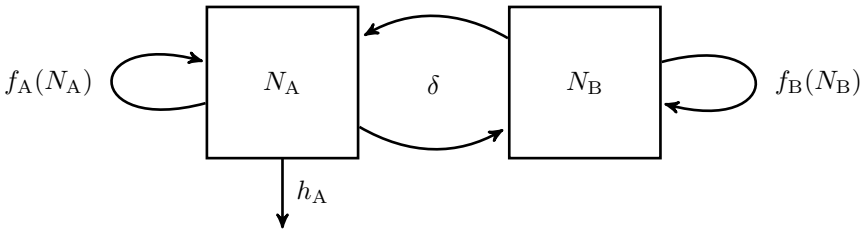

Figure 1: Two-patch model: the subpopulations N_{A} and N_{B} reproduce with growth functions $f_{\mathrm{A}}(N_{\mathrm{A}})$ and $f_{\mathrm{B}}(N_{\mathrm{B}})$, respectively. Individuals can move between the patches with symmetric dispersal (δ). Patch A is subject to proportional harvesting (h_{A}), while patch B is protected.

Discrete-time models are commonly used for populations with seasonal reproduction and the dynamics follow a chronological order. Here, the species

reproduces and is harvested before dispersal occurs:

$$\begin{aligned} N_{\mathrm{A_d}}(t+1) &= (1-\delta_{\mathrm{d}})(1-h_{\mathrm{A_d}})f_{\mathrm{A}_d} + \delta_{\mathrm{d}} f_{\mathrm{B_d}}, \\ N_{\mathrm{B_d}}(t+1) &= (1-\delta_{\mathrm{d}}) f_{\mathrm{B_d}} + \delta_{\mathrm{d}}(1-h_{\mathrm{A_d}}) f_{\mathrm{A_d}}. \end{aligned} \tag{1}$$

The subpopulations $N_{i_{\mathrm{d}}}(t)$ at time step $t \in \mathbb{N}$ disperse with discrete-time dispersal proportion $\delta_{\mathrm{d}} \in [0, 0.5]$ and reproduce with separate growth functions $f_{i_{\mathrm{d}}}$ in patches i =A,B (the subscript "i" will henceforth denote patches A and B). Patch A is subject to proportional harvest with proportion $h_{\mathrm{A_d}} \in [0, 1]$. We have used the subscript "d" to signify the discrete-time setting and the notation $f_{i_{\mathrm{d}}} := f_{i_{\mathrm{d}}}(N_{i_{\mathrm{d}}}(t))$ to simplify the exposition. The yield reads $Y_{\mathrm{d}}(t+1) = h_{\mathrm{A_d}} f_{\mathrm{A_d}}$.

The continuous-time model reads

$$\begin{aligned} \frac{dN_{\mathrm{A_c}}}{dt} &= f_{\mathrm{A_c}} + \delta_{\mathrm{c}}(N_{\mathrm{B_c}} - N_{\mathrm{A_c}}) - h_{\mathrm{A_c}} N_{\mathrm{A_c}}, \\ \frac{dN_{\mathrm{B_c}}}{dt} &= f_{\mathrm{B_c}} + \delta_{\mathrm{c}}(N_{\mathrm{A_c}} - N_{\mathrm{B_c}}), \end{aligned} \tag{2}$$

with subpopulation sizes $N_{i_{\mathrm{c}}}$ at time $t \in \mathbb{R}_+$. A consistent notation is used, where all continuous-time variables and parameters are identified by the subscript "c", distinguishing them from their discrete-time counterparts, with the dispersal rate $\delta_{\mathrm{c}} \geq 0$ and the harvest rate $h_{\mathrm{c}} \geq 0$. The yield reads $Y_{\mathrm{c}}(t) = h_{\mathrm{A_c}} N_{\mathrm{A_c}}(t)$. Whenever parameters or variables are not explicitly labelled with "c" or "d", the statement applies to both time frameworks.

Dispersal is limited within the range of isolation ($\delta = 0$) to *perfect mixing* (the number of individuals in patches A and B is balanced). In discrete time, perfect mixing is reached when the dispersal proportion equals $\delta_{\mathrm{d}} = 0.5$, while in continuous time $\delta_{\mathrm{c}} \to \infty$ leads to a perfectly mixed total population.

Each subpopulation reproduces independently. In the discrete-time model, we employ the Beverton–Holt dynamics

$$f_{\mathrm{d}}(N_{\mathrm{d}}) = \frac{r_{\mathrm{d}} N_{\mathrm{d}}}{1 + (\frac{r_{\mathrm{d}}-1}{K_{\mathrm{d}}}) N_{\mathrm{d}}}. \tag{3}$$

In the continuous-time model, the logistic growth function is used

$$f_{\mathrm{c}}(N_{\mathrm{c}}) = r_{\mathrm{c}} N_{\mathrm{c}} \left(1 - \frac{N_{\mathrm{c}}}{K_{\mathrm{c}}}\right). \tag{4}$$

In both growth functions, r represents the intrinsic growth rate and K denotes the carrying capacity.

All parameters are positive. In the absence of harvest, both patches act as sources, approaching their carrying capacity in isolation. This implies that in both patches the intrinsic growth rate is $r_\mathrm{d} > 1$ in discrete time and $r_\mathrm{c} > 0$ in continuous time. Both growth functions encapsulate intraspecific competition, quantified by $c_\mathrm{d} = \frac{r_\mathrm{d}-1}{K_\mathrm{d}}$ in discrete time and $c_\mathrm{c} = \frac{r_\mathrm{c}}{K_\mathrm{c}}$ in continuous time.

2.2. Proportional harvesting in a single population

This recap of proportional harvesting in a single population introduces effective parameters that incorporate the impact of harvesting into the growth functions. These parameters simplify the model equations and readily show whether these are effective source–source or source–sink dynamics.

In discrete time, the population size of a single population that is subject to proportional harvesting follows

$$N_{t+1_\mathrm{d}} = (1-h_\mathrm{d})\frac{r_\mathrm{d}N_{t_\mathrm{d}}}{1+\frac{r_\mathrm{d}-1}{K_\mathrm{d}}N_{t_\mathrm{d}}} := F_\mathrm{d}(N_{t_\mathrm{d}}). \tag{5}$$

We can rewrite $F_\mathrm{d}(N_{t_\mathrm{d}})$ by including the harvesting parameter into the growth function and identify an effective growth rate and an effective carrying capacity:

$$\begin{aligned}\tilde{r}_\mathrm{d} &= (1-h_\mathrm{d})r_\mathrm{d},\\ \tilde{K}_\mathrm{d} &= K_\mathrm{d}\left(1-\frac{r_\mathrm{d}}{r_\mathrm{d}-1}h_\mathrm{d}\right).\end{aligned}$$

Then Eq. (5) can be written as $N_{t+1_\mathrm{d}} = \tilde{f}_\mathrm{d}(N_\mathrm{d})$ where $\tilde{f}_\mathrm{d}(N_\mathrm{d}) = \frac{\tilde{r}_\mathrm{d}N_\mathrm{d}}{1+\frac{\tilde{r}_\mathrm{d}-1}{\tilde{K}_\mathrm{d}}N_\mathrm{d}}$ is the effective growth function. The asymptotic population size reads

$$N_\mathrm{d}^* = \begin{cases}\tilde{K}_\mathrm{d} & \text{if } h_\mathrm{d} < h_{2_\mathrm{d}},\\ 0 & \text{else,}\end{cases}$$

where $h_{2_\mathrm{d}} = 1-\frac{1}{r_\mathrm{d}}$ represents the critical harvesting threshold. Sustainable harvesting ($h_\mathrm{d} < h_{2_\mathrm{d}}$) leads to the asymptotic yield $Y_\mathrm{d}^*(h_\mathrm{d}) = h_\mathrm{d}\tilde{K}_\mathrm{d}$. Overharvesting ($h_\mathrm{d} > h_{2_\mathrm{d}}$) leads to population extinction and zero yield; additionally, the effective growth rate becomes less than one and the effective carrying capacity becomes negative.

We adopt the same procedure to find effective parameters in continuous time. The differential equation for a single population with proportional harvesting is

$$\frac{dN_\mathrm{c}}{dt} = r_\mathrm{c} N_\mathrm{c}\left(1 - \frac{N_\mathrm{c}}{K_\mathrm{c}}\right) - h_\mathrm{c} N_\mathrm{c} := F_\mathrm{c}(N_\mathrm{c}). \tag{6}$$

The effective parameters read

$$\begin{aligned}\tilde{r}_\mathrm{c} &= r_\mathrm{c} - h_\mathrm{c},\\ \tilde{K}_\mathrm{c} &= K_\mathrm{c}\left(1 - \frac{h_\mathrm{c}}{r_\mathrm{c}}\right).\end{aligned}$$

Then Eq. (6) can be written as $\frac{dN_\mathrm{c}}{dt} = \tilde{f}_\mathrm{c}(N_\mathrm{d})$ where $\tilde{f}_\mathrm{c}(N_\mathrm{c}) = \tilde{r}_\mathrm{c} N_\mathrm{c}\left(1 - \frac{N_\mathrm{c}}{\tilde{K}_\mathrm{c}}\right)$ is the effective growth function. The asymptotic population size read

$$N_\mathrm{c}^* = \begin{cases} \tilde{K}_\mathrm{c} & \text{if } h_\mathrm{c} < h_{2_\mathrm{c}},\\ 0 & \text{else,}\end{cases}$$

where $h_{2_\mathrm{c}} = r_\mathrm{c}$ represents the the critical harvesting rate. When harvesting sustainably ($h_\mathrm{c} < h_{2_\mathrm{c}}$) the asymptotic yield reads $Y_\mathrm{c}^*(h_\mathrm{c}) = h_\mathrm{c}\tilde{K}_\mathrm{c}$ and zero otherwise. In contrast to the discrete-time model, the effective growth rate and the effective carrying capacity become negative when overharvested.

In both time frameworks, intraspecific competition remains uninfluenced by harvesting as harvest terms cancel each other $\tilde{c}_\mathrm{d} = \frac{\tilde{r}_\mathrm{d}-1}{\tilde{K}_\mathrm{d}} = \frac{r_\mathrm{d}-1}{K_\mathrm{d}} = c_\mathrm{d}$ in discrete time and $\tilde{c}_\mathrm{c} = \frac{\tilde{r}_\mathrm{c}}{\tilde{K}_\mathrm{c}} = \frac{r_\mathrm{c}}{K_\mathrm{c}} = c_\mathrm{c}$ in continuous time.

Figure 2 illustrates $\tilde{f}(N)$ for three scenarios: no harvesting (blue), sustainable harvesting (solid red), and overharvesting (dashed red). The effective growth rates can be derived from the slope in the origin and the effective carrying capacity from the intersection with the grey dashed line.

In the two-patch model, if one patch is harvested such that the population would persist in isolation, this case is termed *effective source–source* dynamics. Conversely, when one patch is overharvested to the extent that it would become extinct if isolated, it is referred to as *effective source–sink* dynamics.

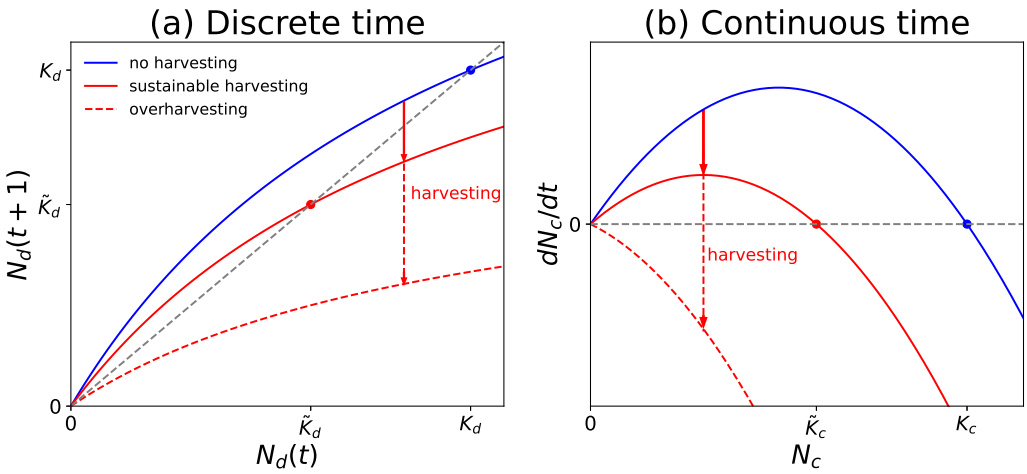

Figure 2: Three qualitative different scenarios resulting from proportional harvesting in (a) discrete-time model with Beverton–Holt growth and (b) continuous time with logistic growth: no harvesting (blue), sustainable harvesting, i.e., effective source dynamics (solid red), and overharvesting, i.e., effective sink dynamics (dashed red). The filled circles mark positive equilibria. The grey dashed line indicates the stationarity condition in each time framework.

3. Asymptotic total population size

In this Section, we analyse the qualitative behaviour of the ATPS in response to increasing dispersal when harvesting one patch. The asymptotic subpopulations sizes are denoted as N_{A}^* and N_{B}^*. We will compare the asymptotic total population size ATPS $= N_{\mathrm{A}}^* + N_{\mathrm{B}}^*$ when the patches are connected to the ATPS when the patches are in isolation. The latter *reference value* is denoted as ATPS_0.

In the effective source–source scenario (i.e., $r_{i_{\mathrm{d}}} > 1, r_{i_{\mathrm{c}}} > 0$), in the absence of dispersal, the equilibrium is given by $\mathrm{ATPS}_0 = \tilde{K}_{\mathrm{A}} + K_{\mathrm{B}}$ for all initial conditions. When connected, a globally stable and unique fixed point emerges within a dispersal range from isolation to perfect mixing (proven by [22] in discrete time and by [27] in continuous time).

Now, let us consider the source–sink scenario where patch A goes extinct in isolation (i.e., $\tilde{r}_{\mathrm{A_d}} < 1, \tilde{r}_{\mathrm{A_c}} < 0$) while patch B remains a source (i.e., $\tilde{r}_{\mathrm{B_d}} > 1, \tilde{r}_{\mathrm{B_c}} > 0$). Without dispersal, the equilibrium is given by $\mathrm{ATPS}_0 = K_{\mathrm{B}}$ for all initial conditions. When connected, a unique positive equilibrium is approached or the ATPS is doomed to extinction. In continuous time,

- the positive equilibrium is approached by all nonzero initial conditions if $|\tilde{r}_{\mathrm{A_c}}| \leq r_{\mathrm{B_c}}$ or if $|\tilde{r}_{\mathrm{A_c}}| > r_{\mathrm{B_c}}$ with $\delta_{\mathrm{c}} < \delta_{\mathrm{crit_c}}$.
- All initial conditions will lead to extinction if $|\tilde{r}_{\mathrm{A_c}}| > r_{\mathrm{B_c}}$ with $\delta_{\mathrm{c}} \geq \delta_{\mathrm{crit_c}}$.

In discrete time,

- the positive equilibrium is approached by all nonzero initial conditions if $2 < \tilde{r}_{\mathrm{A_d}} + r_{\mathrm{B_d}}$ or if $2 \geq \tilde{r}_{\mathrm{A_d}} + r_{\mathrm{B_d}}$ with $\delta_{\mathrm{d}} < \delta_{\mathrm{crit_d}}$.
- All initial conditions will lead to extinction if $2 \geq \tilde{r}_{\mathrm{A_d}} + r_{\mathrm{B_d}}$ with $\delta_{\mathrm{d}} \geq \delta_{\mathrm{crit_d}}$.

We identify a total of five distinct response scenarios of the ATPS to increasing dispersal that arise in both discrete-time and continuous-time frameworks. Here, we will provide a concise overview of these response scenarios; detailed information and proofs can be found in Appendix A (discrete time) and Appendix B (continuous time) . We will describe the impact of dispersal on the ATPS as *beneficial* if the ATPS exceeds the reference value ATPS_0 or *detrimental* if it falls below.

MB *Monotonically beneficial* (see Fig. 3(a)): The effect of dispersal is always beneficial, and the ATPS increases monotonically with increasing dispersal.

UB *Unimodally beneficial* (see Fig. 3(b)): The effect of dispersal is beneficial for all dispersal intensities, with the ATPS increasing until it reaches a global maximum; beyond that point, the ATPS begins to decrease.

BTD *Beneficial turning detrimental* (see Fig. 3(c)): The ATPS is positive for all dispersal intensities. Low dispersal intensity has a beneficial effect, but once a certain threshold is exceeded, the ATPS falls below the reference value, turning the effect detrimental.

MD *Monotonically detrimental* (see Fig. 3(d)): The ATPS is positive for all dispersal intensities. The effect of dispersal is always detrimental and the ATPS decreases monotonically with increasing dispersal.

E *Extinction* (see Fig. 3(e)): The ATPS decreases monotonically as dispersal increases and drops to zero at a certain dispersal threshold.

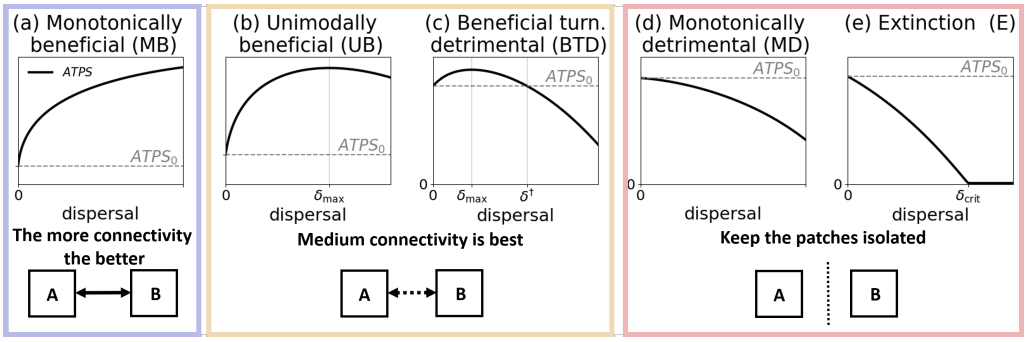

Figure 3: Sketch of each response scenario of the asymptotic total population size (ATPS) to dispersal in discrete and continuous time. The solid line represents the ATPS when dispersal varies from isolation to perfect mixing. The dashed grey line shows the reference value of the ATPS_0. There are three key dispersal values: $\delta_{\max}$ leading to maximum ATPS, the threshold $\delta^\dagger$ at which dispersal impact turns from beneficial to detrimental, and the critical dispersal value δ_{crit} where the ATPS equals zero. The five response scenarios can be classified into three categories "The more connectivity the better", "Medium connectivity is best" and "Keep the patches isolated".

As can be seen in Fig. 3, we classified the response scenarios into three key statement about connectivity: "The more connectivity the better", "Medium connectivity is best" and "Keep the patches isolated". In the following, we present parameter conditions for the qualitatively different response scenarios, delineate their parameter domains and provide a mechanistic interpretation in different parameter scenarios.

3.1. Harvesting the small patch

We assume the smaller patch A is subject to proportional harvesting, while the larger patch B is designated as the protected patch.

3.1.1. Effective source–sink dynamics

Here, we determine the conditions for the five response scenarios through a graphical analysis applicable to both discrete– and continuous–time frameworks. In the effective source–sink scenario, the harvested patch A goes extinct $N_{\mathrm{A}}^{*} = 0$ and the protected patch B approaches its carrying capacity $N_{\mathrm{B}}^{*} = K_{\mathrm{B}} > 0$ in isolation. Therefore, the reference value becomes $\mathrm{ATPS}_0 = K_{\mathrm{B}}$.

The five response scenarios can be distinguished using four criteria (C1 - C4) outlined in Tab. 1. The table provides precise conditions for each criterion and associates them with specific response scenarios, applicable to both continuous- and discrete-time models. The origin of these conditions will be explained in detail in the following graphical analysis.

Graphical analysis. This graphical approach explains the origin of the parameter conditions of each response scenario from Table 1. Consider local growth in each patch in the discrete-time setting in Fig. 4(a) and in the continuous-time setting Fig. 4(b). In discrete time, growth is defined by subtracting the population size in next iteration step from the the current population size

$$G_{\mathrm{d}}(N) = f_{\mathrm{d}}(N_{\mathrm{d}}) - N_{\mathrm{d}},$$

while in continuous time growth is simply given by

$$G_{\mathrm{c}}(N_{\mathrm{c}}) = f_{\mathrm{c}}(N_{\mathrm{c}}).$$

Table 1: Parameter conditions for the five response scenarios within an (effective) source–sink environment derived from the graphical analysis. These conditions apply to both the discrete-time model with Beverton–Holt growth and the continuous-time model with logistic growth, except that the monotonically detrimental response scenario does not occur in continuous time. The criteria are based on the growth of each patch $G_{\mathrm{A}}(N_{\mathrm{A}})$ and $G_{\mathrm{B}}(N_{\mathrm{B}})$ and the asymptotic population size of both patches when perfectly mixed N_P^*. Further explanation is provided in the text.

<table>
<tr><th rowspan="2">Response scenarios</th><th colspan="4">Criteria</th></tr>
<tr><th>Positive equilibrium exists at perfect mixing (C1)</th><th>Positive slope at zero dispersal (C4)</th><th>Beneficial at perfect mixing (C2)</th><th>Positive slope at perfect mixing (C3)</th></tr>
<tr><td>MB
Monotonically beneficial</td><td rowspan="4">if
$\lvert G'_{\mathrm{A}}(0)\rvert < \lvert G'_{\mathrm{B}}(0)\rvert$</td><td rowspan="3">if
$\lvert G'_{\mathrm{A}}(0)\rvert < \lvert G'_{\mathrm{B}}(K_{\mathrm{B}})\rvert$</td><td rowspan="2">if
$N_P^* > \frac{K_{\mathrm{B}}}{2}$</td><td>if
$\lvert G'_{\mathrm{A}}(N_P^*)\rvert \leq \lvert G'_{\mathrm{B}}(N_P^*)\rvert$</td></tr>
<tr><td>UB
Unimodally beneficial</td><td rowspan="2">else</td></tr>
<tr><td>BTD
Beneficial turning detrimental</td><td>else</td></tr>
<tr><td>MD
Monotonically detrimental</td><td>else</td><td></td></tr>
<tr><td>E
Extinction</td><td>else</td><td></td><td></td><td></td></tr>
</table>

In patch A, we utilize the effective growth function $\tilde{f}_{\mathrm{A}}(N_{\mathrm{A}})$ to incorporate the impact of harvesting. We express the discrete-time model (1) and continuous-time model (2) using the total population size:

$$\begin{aligned} N_{\mathrm{A}_{t+1,d}} + N_{\mathrm{B}_{t+1,d}} &= \tilde{f}_{\mathrm{A_d}} + f_{\mathrm{B_d}}, \\ \frac{d}{dt}(N_{\mathrm{A_c}} + N_{\mathrm{B_c}}) &= \tilde{f}_{\mathrm{A_c}} + f_{\mathrm{B_c}}, \end{aligned} \tag{7}$$

and the difference in population sizes between the patches:

$$\begin{aligned} N_{\mathrm{B}_{t+1,d}} - N_{\mathrm{A}_{t+1,d}} &= (1-2\delta_{\mathrm{d}})(f_{\mathrm{B_d}} - \tilde{f}_{\mathrm{A}_d}), \\ \frac{d}{dt}(N_{\mathrm{B_c}} - N_{\mathrm{A_c}}) &= (f_{\mathrm{B_c}} - \tilde{f}_{\mathrm{A_c}}) + 2\delta_{\mathrm{c}}(N_{\mathrm{A_c}} - N_{\mathrm{B_c}}). \end{aligned} \tag{8}$$

where we have used the notation$f_i := f_i(N_i)$ to simplify the exposition. At equilibrium, Eq. (7) in both discrete and continuous time leads to

$$G_{\mathrm{A}}(N_{\mathrm{A}}^*) + G_{\mathrm{B}}(N_{\mathrm{B}}^*) = 0, \tag{9}$$

for equilibrium values N_{A}^* and N_{B}^* assuming $N_{\mathrm{A}}^* \neq N_{\mathrm{B}}^*$. Eq. (8) leads to

$$\frac{G_{\mathrm{B}}(N_{\mathrm{B}}^*) - G_{\mathrm{A}}(N_{\mathrm{A}}^*)}{N_{\mathrm{B}}^* - N_{\mathrm{A}}^*} = \begin{cases} \frac{2\delta_{\mathrm{d}}}{1-2\delta_{\mathrm{d}}} & \text{in discrete time, and} \\ 2\delta_{\mathrm{c}} & \text{in continuous time.} \end{cases} \tag{10}$$

There are infinitely many pairs of populations sizes N_{A}^* and N_{B}^* for which Eq. (9) and (10) hold, e.g. those connected by the black arrows in Fig. 4. The first equilibrium condition Eq. (9) means that the total population size remains constant when the growth of patch B compensates the decline in patch A, so whenever the vertical distances to the horizontal axis of G_{A} and G_{B} are equal. The second equilibrium condition Eq. (8) imposes the slope of the arrow connecting the two equilibrial points $(N_{\mathrm{A}}^*, G_{\mathrm{A}}(N_{\mathrm{A}}^*))$ and $(N_{\mathrm{B}}^*, G_{\mathrm{B}}(N_{\mathrm{B}}^*))$ to the given values of Eq. (10).

Using this graphical approach, we can derive the following insights.

- When isolated ($\delta = 0$), the population in patch A goes extinct ($N_{\mathrm{A}}^* = 0$) while patch B's population approaches its carrying capacity ($N_{\mathrm{B}}^* = K_{\mathrm{B}}$). The slope of the line connecting the pair $(0, 0)$ and $(K_{\mathrm{B}}, 0)$ equals zero as shown in Eq. (10).

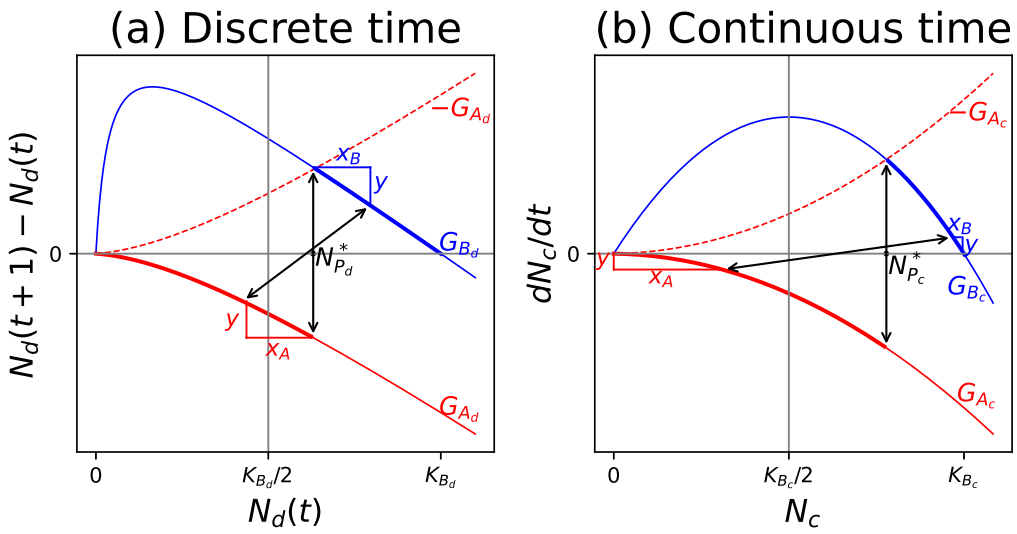

Figure 4: The growth functions of patches A (red) and B (blue) using (a) the Beverton–Holt function in discrete time and (b) the logistic function in continuous time in the monotonically beneficial response scenario. Infinitely many equilibrium pairs (N^*_{A},N^*_{B}) can be found by connecting two points on the bold segments of each patch, e.g. those connected by the black arrows. Two equilibrium conditions must be satisfied: 1) same vertical axis distance for G_{A} and G_{B}, and 2) connecting arrows with slope $\frac{2\delta_{\mathrm{d}}}{1-2\delta_{\mathrm{d}}}$ in discrete time and $2\delta_{\mathrm{c}}$ in continuous time. The vertical arrow indicates perfect mixing (where $N^*_{\mathrm{A}} = N^*_{\mathrm{B}} := N^*_{\mathrm{P}}$) found at the intersection of G_{B} and $-G_{\mathrm{A}}$. The intersections of the connecting arrows with the horizontal axis denotes half of the ATPS for that particular pair. The parameter values for (a) are $r_{\mathrm{A_d}} = 2$, $r_{\mathrm{B}_d} = 26$ $K_{\mathrm{A_d}} = 40$, $K_{\mathrm{B_d}} = 60$, $h_{\mathrm{d}} = 0.55$ and for (b) $r_{\mathrm{A}_c} = 2$, $r_{\mathrm{B}_c} = 11$ $K_{\mathrm{A}_c} = 40$, $K_{\mathrm{B}_c} = 60$, $h_{\mathrm{c}} = 2.1$. Both scenarios correspond to the monotonically beneficial response scenario.

- When perfectly mixed ($\delta_{\mathrm{d}} = 0.5, \delta_{\mathrm{c}} \to \infty$), the population sizes in patches A and B equalise ($N^*_{\mathrm{A}} = N^*_{\mathrm{B}} := N^*_{\mathrm{P}}$). The equilibrium population sizes can be determined where the growth functions G_{B} and $-G_{\mathrm{A}}$ intersect. The connecting vertical has an infinite slope, as shown in Eq. (10).

Combining these two scenarios and considering dispersal ranging from zero to perfect mixing, all possible equilibrium population pairs must lie on the thickly marked parts of their growth functions. This constitutes a graphical procedure to find the equilibrium population sizes in the two patches: find a pair of points where $G_{\mathrm{B}}(N_{\mathrm{B}}) = -G_{\mathrm{A}}(N_{\mathrm{A}})$ and connect them by a line with the slope associated with dispersal.

Now, we can derive the four criteria introduced in Tab. 1.

C1 **Positive equilibrium exists at perfect mixing.** A positive ATPS equilibrium at perfect mixing (i.e., $N_{\mathrm{P}}^* > 0$) exists if and only if there is an intersection between $-G_{\mathrm{A}}$ and G_{B} in the positive quadrant. This intersection occurs when the slope of $-G_{\mathrm{A}}$ (red dotted line) is less steep than the slope of G_{B} (blue solid line) in the origin, i.e., $|G'_{\mathrm{A}}(0)| < |G'_{\mathrm{B}}(0)|$. If this condition is not met, both populations will go extinct at perfect mixing because there will be no intersection except in the origin where $-G_{\mathrm{A}} = G_{\mathrm{B}}$.

The arrow connecting an equilibrium pair intersects the horizontal axis, and the N value at this intersection represents half of the ATPS for that significant pair. When this value exceeds half of the reference value $K_{\mathrm{B}}/2$, the effect of dispersal on the ATPS is beneficial. In contrast, if the value is less than $K_{\mathrm{B}}/2$, the impact of dispersal is detrimental.

C2 **Beneficial at perfect mixing.** Half of the ATPS at perfect mixing is represented by N_{P}^*. If N_{P}^* exceeds $K_{\mathrm{B}}/2$, the ATPS exceeds the reference value, indicating a beneficial effect. Otherwise, the effect on the ATPS is detrimental at perfect mixing.

C3 **Positive slope at perfect mixing.** An equilibrium pair with dispersal close to perfect mixing leads to a smaller ATPS than dispersal at perfect mixing. Figure 4(a) shows a slope triangle from N_{P}^* (at perfect mixing) to an equilibrium pair close to perfect mixing. The associated arrow intersects the horizontal axis to the left of N_{P}^* indicating a smaller ATPS close to perfect mixing. The vertical component y of the slope triangle must be equal for both patches (see Eq. (9)). Therefore, increasing the slope at $G_i(N_{\mathrm{P}}^*)$ decreases the associated horizontal component x_i. If $x_{\mathrm{A}} > x_{\mathrm{B}}$, the intersection of an equilibrium pair close to perfect mixing occurs to the left of N_{P}^*, implying that the ATPS increases locally when $|G'_{\mathrm{A}}(N_{\mathrm{P}}^*)| < |G'_{\mathrm{B}}(N_{\mathrm{P}}^*)|$.

C4 **Positive slope at zero dispersal.** See Fig. 4(b), if the slope of G_{A} in the origin is smaller than the slope of G_{B} at K_{B}, then the intersection is positioned to the right of $K_{\mathrm{B}}/2$. In other words, if $|G'_{\mathrm{A}}(0)| < |G'_{\mathrm{B}}(K_{\mathrm{B}})|$, then the ATPS increases when dispersal is introduced into an isolated system.

Using these four criteria, we can identify the five different response scenarios as introduced in Tab. 1.

Comparison of discrete and continuous time. This graphical approach has been applied analogously in both discrete- and continuous-time frameworks. When calculating the exact parameter conditions for each time setting, we find that there is no MD response scenario in the continuous-time source–sink model.

The boundaries of the MD response scenario are determined by criteria C1 and C4:

- In discrete time, C1 ensures that the ATPS remains persistent for all dispersal values $\delta_\mathrm{d} \in [0, 0.5]$ if $2 \leq \tilde{r}_{\mathrm{A_d}} + r_{\mathrm{B_d}}$. C4 states that if $1 > \tilde{r}_{\mathrm{A_d}} r_{\mathrm{B_d}}$ the ATPS response is detrimental when dispersal is introduced to an isolated system. Thus, the MD scenario is defined by the condition $2 - r_{\mathrm{B_d}} \leq \tilde{r}_{\mathrm{A_d}} < 1/r_{\mathrm{B_d}}$.

- In continuous time, C1 ensures that the ATPS remains persistent for all dispersal values $\delta_\mathrm{d} > 0$ if $|\tilde{r}_{\mathrm{A_c}}| < |r_{\mathrm{B_c}}|$. C4 states for the exact same condition $|\tilde{r}_{\mathrm{A_c}}| < |r_{\mathrm{B_c}}|$ that the ATPS response is detrimental when introducing dispersal to an isolated system. Consequently, if the effect of dispersal is detrimental when introducing dispersal the ATPS will go extinct at perfect mixing. Thus, the monotonic detrimental response scenario does not exist in continuous time.

This discrepancy arises from the shape of the logistic growth function, which forms a symmetric parabola due to its linear density dependence (see Fig. 4(b)). This symmetry implies that the slope of the growth function has the same absolute value at the origin and at its carrying capacity in the source patch leading to equal conditions from C1 and C4.

3.1.2. Effective source–source dynamics

If harvesting in patch A does not surpass the critical harvest threshold, above which the population faces extinction, we can consider an effective source–source scenario. In contrast to [14], we do not define a source as a net exporter, but in such a way that both source patches persist in isolation approaching the reference value ATPS $= \tilde{K}_\mathrm{A} + K_\mathrm{B}$. The two-patch model characterised by source–source dynamics was extensively analysed by [22].

We expand on their categorisation of response scenarios to include harvesting effects.

Within the effective source–source scenario, there are the same response scenarios as in the effective source–sink scenario, except for the extinction scenario. Table 2 provides a synthesis of the parameter conditions, encompassing both continuous-time and discrete-time models. The parameter conditions are delineated in terms of (effective) intrinsic growth rates, (effective) carrying capacities, and intraspecific competition coefficients, the latter being ratios of the former two parameters.

Table 2: Parameter conditions for the four response scenarios within an (effective) source–source scenario. The threshold value of $\tilde{\kappa} > 1$ delineates the degree to which intraspecific competition in patch B must exceed that of patch A to prompt the monotonically beneficial response scenario. In discrete time the threshold is denoted as $\tilde{\kappa}_{\mathrm{d}} = \frac{r_{\mathrm{B}}+\sqrt{\tilde{r}_{\mathrm{A}} r_{\mathrm{B}}}-2}{\tilde{r}_{\mathrm{A}}+\sqrt{\tilde{r}_{\mathrm{A}} r_{\mathrm{B}}}-2}$ and in continuous time as $\tilde{\kappa}_{\mathrm{c}} = \frac{\tilde{r}_{\mathrm{A_c}}+3r_{\mathrm{B_c}}}{r_{\mathrm{B_c}}+3\tilde{r}_{\mathrm{A_c}}}$.

<table>
<tr><th>Response Scenarios</th><th colspan="3">Criteria</th></tr>
<tr><td>MB
Monotonically beneficial</td><td rowspan="4">$\tilde{K}_{\mathrm{A}} < K_{\mathrm{B}}$</td><td rowspan="3">$\tilde{r}_{\mathrm{A}} < r_{\mathrm{B}}$</td><td>$\tilde{\kappa} c_{\mathrm{A}} < c_{\mathrm{B}}$</td></tr>
<tr><td>UB
Unimodally beneficial</td><td>$c_{\mathrm{A}} < c_{\mathrm{B}} < \tilde{\kappa} c_{\mathrm{B}}$</td></tr>
<tr><td>BTD
Beneficial turn. detrimental</td><td>$c_{\mathrm{B}} < c_{\mathrm{A}}$</td></tr>
<tr><td>MD
Monotonically detrimental</td><td>$\tilde{r}_{\mathrm{A}} \leq r_{\mathrm{B}}$</td><td></td></tr>
</table>

3.1.3. Parameter domains of response scenarios

Figure 5 shows the parameter domains of the response scenarios when varying the intensity of the harvest h_{A} in the smaller patch A to investigate the impact of increasing the harvest. We also vary the intrinsic growth rate r_{B} of the larger patch B, so that all response scenarios are represented. All other parameters remain constant. Figure 5(a) and (b) can be divided into two parts: As long as the harvesting intensity is below patch A's critical harvest value h_2, the system remains in an effective source–source scenario; left to the dashed vertical line and to the right, the system can be classified as an effective source–sink scenario.

Within the effective source–source scenario ($h \in [0, h_2]$), the parameter conditions are outlined in Tab. 2. We can observe the three boundaries shifting as harvesting increases:

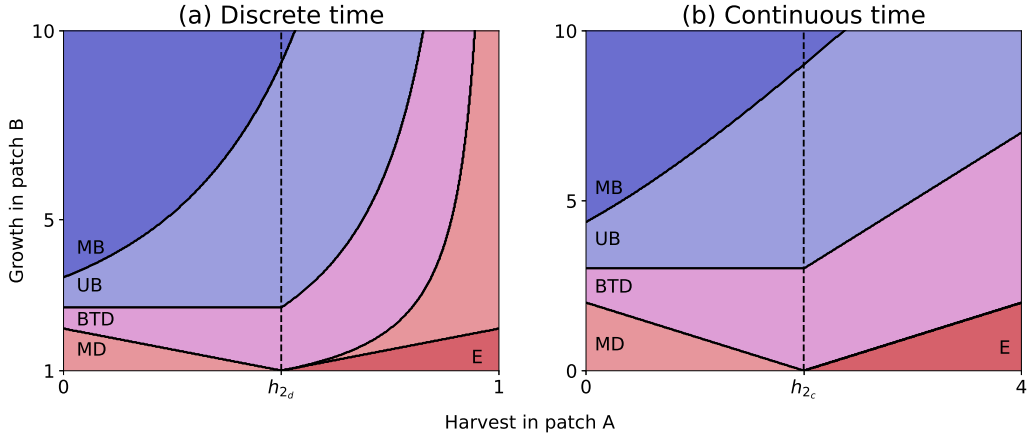

Figure 5: Harvesting the small patch: the parameter domains for the five response scenarios in (a) discrete time and (b) continuous time. The response scenarios are MB (monotonically beneficial), UB (unimodally beneficial), BTD (beneficial turning detrimental), MD (monotonically detrimental) and E (extinction). The parameter conditions of the response scenarios in the source–source scenario ($h \in [0, h_2]$) are defined in Tab. 2 and in the source–sink scenario ($h > h_2$) are defined by criteria C1-C4 in Tab. 1. The parameter values are $r_\mathrm{A} = 2$, $K_\mathrm{A} = 40$, $K_\mathrm{B} = 60$.

- The MD response scenario emerges as long as $\tilde{r}_\mathrm{A} \leq r_\mathrm{B}$. At zero harvesting, this boundary occurs at $\tilde{r}_\mathrm{A} = r_\mathrm{B} = 2$. Harvesting linearly reduces the intrinsic growth rate to $\tilde{r}_\mathrm{A} = (1 - h_\mathrm{A}) r_\mathrm{A}$. Consequently, the boundary between response scenarios MD and BTD decreases linearly with increasing harvest intensity. This linear decrease continues until the critical harvest value (h_2) is reached. Then, the effective intrinsic growth rate equals the r–bifurcation point of patch A ($\tilde{r}_{\mathrm{A_d}} = 1, \tilde{r}_{\mathrm{A_c}} = 0$).

- The boundary between the BTD and UB response scenarios depends solely on the values of intraspecific competition which remain unchanged under harvesting. Thus, there is no boundary shift due to harvesting in the source–source scenario as depicted as a constant line in Fig. 5.

- The boundary separating the response scenarios MB and UB is defined by the threshold value $\tilde{\kappa}$. When $\tilde{\kappa} c_\mathrm{A} < c_\mathrm{B}$, we are in the MB response scenario. However, as $\tilde{r}_\mathrm{A}$ decreases due to harvesting, $\tilde{\kappa}$ increases, causing the boundary to shift in favour of the UB response scenario (refer to Table 2 for the parameter conditions and exact $\tilde{\kappa}$ definition).

The effective source–source scenarios appear qualitatively similar in the discrete-

time and continuous-time settings. The boundary between the MB and UB response scenarios differs due to the distinct formulations of $\tilde{\kappa}$ and intraspecific competition formulation.

If the harvest value exceeds the critical harvest value of patch A ($h > h_2$), there is an effective source–sink environment with parameter conditions outlined in Tab. 1. Recall that the reference value is now equal to the carrying capacity of patch B exclusively. Whenever the ATPS exceeds the carrying capacity (that is, beneficial effect), a rescue effect occurs from protected patch B to harvested patch A. As harvesting increases and the intrinsic growth rate in the larger patch B decreases, the response scenarios transition stepwise from MB to E (excluding MD in the continuous-time setting).

In discrete time, total population extinction occurs under perfect mixing when the combined intrinsic growth rates of both patches do not exceed the threshold of $2 \leq \tilde{r}_{\mathrm{A_d}} + r_{\mathrm{B_d}}$. The bifurcation point of the intrinsic growth rate, leading to extinction, is 1; therefore, both patches must achieve a combined growth rate of at least 2. Since $\tilde{r}_{\mathrm{A_d}}$ is limited to the range $[0, 1)$ due to harvesting, the protected patch B must be sufficiently strong to compensate and exceed the threshold.

In continuous time, the bifurcation point of the intrinsic growth is zero. Therefore, extinction at perfect mixing arises whenever the sink is stronger than the source: $|\tilde{r}_{\mathrm{A_c}}| < |r_{\mathrm{B_c}}|$.

3.2. Harvesting the large patch

In this Section, we investigate the scenario where the harvested patch A is the one with the larger carrying capacity and the smaller patch B is protected.

Figure 6 shows the parameter domains for this case. Similar to Fig. 5, we vary the intrinsic growth rate of the protected patch B and the harvest intensity in patch A. We find similar parameter domains in the effective source–sink region but distinct characteristics emerge in the effective source–source scenario, particularly for low harvesting values.
Figure 6 can be divided into three ranges of harvesting values:

- Harvesting the effectively larger patch, that is, $h \in [0, h_1]$: the effective carrying capacity of the initially larger patch A is diminished by harvesting, reaching a point where it becomes first equal to and then less than the carrying capacity of the protected patch B. This critical

juncture is denoted in the figure by h_1, where $K_{\mathrm{B_d}} = \tilde{K}_{\mathrm{A_d}}$. To the left of this threshold, patch A remains effectively the larger patch. As introduced in Tab. 2, the mathematical analysis of the effective source–source scenario assumes one patch to be larger than the other one; if the ratio is inverted, all conditions are also reversed.

- Harvesting the effectively smaller patch in effective source–source dynamics, that is, $h \in (h_1, h_2)$: When crossing h_1, harvesting effectively turns the initially larger patch A into the smaller patch, leading to analogous qualitative behaviours observed when harvesting the initially smaller patch. Consequently, the response scenarios are perfectly point reflected at h_1.

- Harvesting the effectively smaller patch in source–sink dynamics, i.e., $h_2 < h$: as harvesting is further increased, the harvested patch becomes a sink as harvesting reaches the critical harvest threshold h_2.

3.3. Mechanistic interpretation

The parameter conditions for the five response scenarios are not only mathematically compelling but also biologically crucial, as they can significantly enhance our understanding of population dynamics in spatially fragmented landscapes. To transform these analytical insights into effective management strategies, it is essential to provide a biological interpretation and a clear explanation of the underlying biological mechanisms. In the following, we will explore these mechanisms in detail to explain the implications of the model.

3.3.1. Harvesting the effectively larger patch

If ($h \in [0, h_1]$), there is a net migration from the larger harvested patch A to the smaller protected patch B. Figure 7(d) shows that as dispersal increases, the population size in patch B (blue) grows, while the population in patch A (red) decreases. This trend continues until perfect mixing is reached, where both patches harbour populations of equal size (the yield in Fig. 7 is discussed in Sec. 4). In this region, Fig. 6 illustrates a shift from the UB to the MB response scenarios and from the BTD to the MD response scenario as harvesting increases:

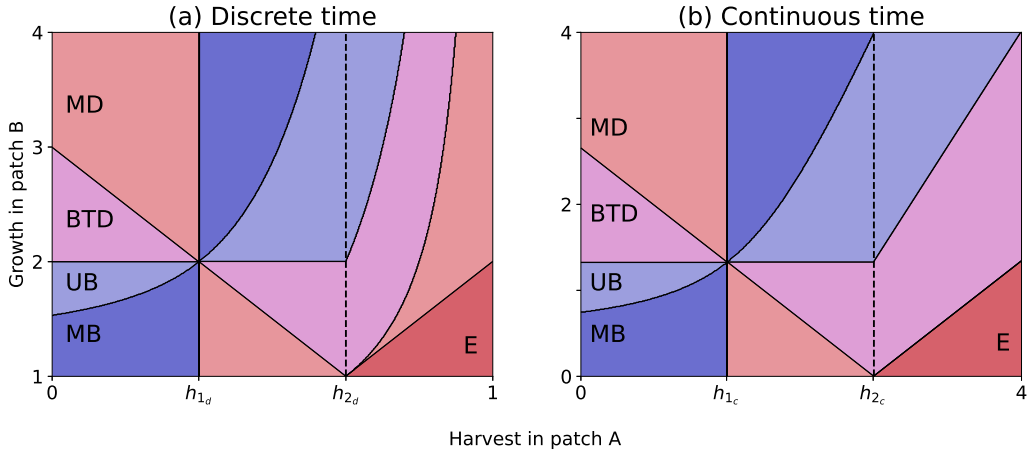

Figure 6: Harvesting the large patch: the parameter domains for the five response scenarios in (a) discrete time and (b) continuous time. The response scenarios are MB (monotonically beneficial), UB (unimodally beneficial), BTD (beneficial turning detrimental), MD (monotonically detrimental) and E (extinction). There are three qualitatively different harvesting ranges: Harvesting the effectively larger patch in effective source–source dynamics ($h \in [0, h_1]$), Harvesting the effectively smaller patch in effective source–source dynamics ($h \in [h_1, h_2]$), Harvesting the effectively smaller patch in effective source–sink dynamics ($h \in [h_2, \infty)$). The parameter conditions of the response scenarios in the effective source–source scenario are given by Tab. 2 and in the effective source–sink scenario are given by criteria C1–C4 in Tab. 1. The effective carrying capacity of the harvested patch A becomes equal to the carrying capacity of the protected patch B at h_1, where $K_{\mathrm{B_d}} = \tilde{K}_{\mathrm{A_d}}$. The parameter values read for (a) $r_{\mathrm{A_d}} = 3$, $K_{\mathrm{A_d}} = 60$, $K_{\mathrm{B_d}} = 30$ and for (b) $r_{\mathrm{A_c}} = 2.67$, $K_{\mathrm{A_c}} = 60$, $K_{\mathrm{B_c}} = 30$.

- Shift from BTD to MD: within the BTD response scenario, the larger patch has the higher growth rate, so that the larger patch is more likely to be overcrowded and benefits from leaving individuals due to dispersal until a certain dispersal threshold is reached. Increasing harvesting in patch A leads to smaller effective growth in the harvested patch; therefore, the smaller protected patch now facilitates the higher growth, leading to overcrowding in the protected patch as dispersal brings in additional individuals. So that, the response scenario shifts from BTD to MD.

- Shift from UB to MB: within the UB response scenario, the larger patch has the higher growth rate, and dispersal helps to reduce overcrowding in the large patch by moving individuals to the smaller patch. However, high dispersal values may be excessive, as a large number of individuals can cause overcrowding within the protected patch. Introducing harvesting in the larger patch reduces the population size difference between the patches, leading to fewer individuals migrating to the smaller patch. As a result, the smaller patch does not overcrowd as quickly, expanding the range of parameters for the MB response scenario.

3.3.2. Harvesting the effectively smaller patch in source–source dynamics

If $h \in [h_1, h_2]$, there is a net migration from the effectively larger protected patch B to the smaller harvested patch A. Figure 7(a) shows that as dispersal increases, the population in patch A (red) grows, while the population in the protected patch B (blue) declines. The domains of the response scenarios are reversed in contrast to the case when the large patch is harvested, resulting in a point reflection. Figure 6 illustrates a shift from MD to BTD and from MB to UB response scenario as harvesting increases.

- Shift from MD to BTD: As discussed above, the MD response scenario emerges if the smaller patch has a higher intrinsic growth rate, so an increase in dispersal results in additional individuals inhabiting the already crowded patch. The introduction of harvesting in the effectively smaller patch A with higher intrinsic growth reduces the population size and relaxes the crowded conditions leading to a shift to the BTD response scenario.

- Shift from MB to UB: In the MB response scenario, the larger protected patch B has a higher intrinsic growth. Dispersal helps reduce

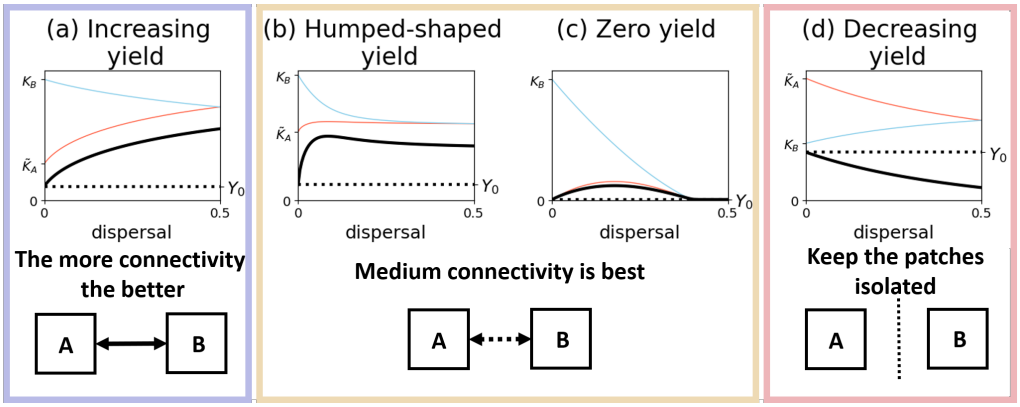

Figure 7: Qualitative behaviour of the asymptotic yield (black) and the asymptotic subpopulation sizes for patch A (red) and patch B (blue) for four different parameter scenarios. The yield under isolation, denoted as Y_0, is marked with a black dotted line. Parameter values in discrete time as in Fig. 6(a) with (a) Decreasing yield with $r_{\mathrm{B_d}} = 4$ and $h_{\mathrm{A_d}} = 0.1$, (b) increasing yield with $r_{\mathrm{B_d}} = 4$ and $h_{\mathrm{A_d}} = 0.4$, (c) humped-shaped yield with $r_{\mathrm{B_d}} = 1.1$ and $h_{\mathrm{A_d}} = 0.47$ and (d) humped-shaped yield leading to zero yield with $r_{\mathrm{B_d}} = 1.4$ and $h_{\mathrm{A_d}} = 0.75$. The model was simulated for 500 time steps and only the last values are plotted. We chose K_A and K_B as initial conditions for subpopulations A and B, respectively.

overcrowding in patch B by moving individuals to the smaller patch A. With the introduction of harvesting, patch A is reduced, sothat the difference in population sizes increases. Therefore, the amount of moving individuals increases and high dispersal values diminish the beneficial effect on the ATPS due to overcrowding in the small harvested patch. As a consequence, the system shifts to the UB response scenario.

The increasing parameter domains of the humped–shaped response scenarios UB and BTD suggest that, within this range, a specific dispersal value between isolation and perfect mixing emerges as the favoured option for achieving the most beneficial outcomes.

3.3.3. Harvesting the effectively smaller patch in source–sink dynamics

If $h_2 < h$, there exists a rescue effect of the effective sink whenever there is a beneficial response of the ATPS. In the MB response scenario, the large growth in patch B is sufficiently strong to offset the decline in patch A resulting from harvesting. Conversely, in all other response scenarios, large dispersal values consistently diminish the ATPS. The weaker the growth in

source patch B, the more detrimental the response scenario becomes. Generally, a detrimental effect can be named *negative sink effect*, where the ATPS falls below the reference value (ATPS $= K_{\mathrm{B}}$). This implies that, through harvesting, the smaller patch A essentially depletes resources from patch B. The weaker source patch B, the more unfavourable the outcome for the ATPS. If the intrinsic growth rate of source patch B is diminished to such an extent that it cannot balance the effective intrinsic growth rate of sink patch A, both populations face extinction. Consequently, harvesting solely from the smaller patch can culminate in complete extinction of both patches.

4. Total asymptotic yield

We will compare the asymptotic yield, $Y^*(N_{\mathrm{A}}^*)$ when the patches are connected to the asymptotic yield when the patches are isolated. This *reference value* is denoted as Y_0.

In this Section, we explore the qualitative behaviour of the asymptotic yield in response to increasing dispersal when harvesting occurs either in the larger patch or the smaller patch. Since the yield is directly proportional to the size of the harvested subpopulation, our focus is on the subpopulation sizes rather than the total population size.

Figure 7 presents the asymptotic subpopulation sizes for the harvested patch A (red), the protected patch B (blue), the asymptotic yield (black) and the reference value yield at isolation Y_0 (black dotted) for four parameter scenarios in discrete time (the results for the continuous-time system are qualitatively similar). In an effective source–sink environment, the yield is consistently compared to zero, as without dispersal the harvested patch would go extinct, resulting in zero yield. As in Fig. 3, we classify the yield behaviours into three categories: "The more connectivity the better", "Medium connectivity is best" and "Keep the patches isolated".

Figure 7(a, b, c) illustrate scenarios where the harvested patch A is smaller than protected patch B, resulting in net dispersal from patch B to patch A. Following from this assumption, we found three qualitatively distinct behaviours of the asymptotic yield in response to increasing dispersal.

- *Increasing yield* (see Fig. 7(a)): Patch A's subpopulation size and catch increase monotonically due to positive net dispersal towards patch A.

- *Humped-shaped yield* (see Fig. 7(b)): As harvest intensity increases, the effective carrying capacity in patch A decreases, leading to a larger

population size difference between the patches. Then, low dispersal has a high impact on the effectively small patch causing a substantial increase. However, as dispersal increases, this effect diminishes due to the decreasing of patch B, which is unable to compensate for the missing individuals. Then, high dispersal eventually even decreases the asymptotic yield.

- *Zero yield* (see Fig. 7(c)): Patch A and the total population go extinct at a certain dispersal value, resulting in catch decreasing to zero, which is similar to the Extinction response scenarios of the total population size.

Figure 7(d) shows the scenario in which the harvested patch A has the larger carrying capacity, leading to

- *Decreasing yield*: Due to the net dispersal from patch A to patch B, patch A loses individuals through both harvesting and dispersal, leading to a monotonic decrease in yield as dispersal increases.

Figure 8 depicts the parameter domains of the four qualitative behaviours of yield to increasing dispersal where (a) the harvested patch has the smaller effective carrying capacity using the same parameter values as in Fig. 5(a), and (b) the harvested patch has the larger effective carrying capacity using the parameter values as in Fig. 6(a). When comparing the parameter domains of the ATPS response scenarios presented in Figures 5(a) and 6(a) with those of the yield behaviours, it becomes apparent that they do not align - for instance, the parameter domains for increasing yield and the MB response scenario differ significantly. The E response scenario and zero yield scenario are a notable exception, as an extinct population naturally results in zero yield.

Harvesting the small patch leads to increasing yield, as long as the growth in the protected patch is strong and harvesting is modest. Strong harvesting and a slowly growing protected patch can lead to detrimental effects on the yield if dispersal values are high because the protected patch B can not compensate the loss due to harvesting.

When harvesting the large patch, dispersal has a detrimental effect on the asymptotic yield as the net migration flows from the harvested patch towards the protected patch. Such that the harvested patch is loosing individuals due to dispersal and harvesting. Once the effective carrying capacity of patch A

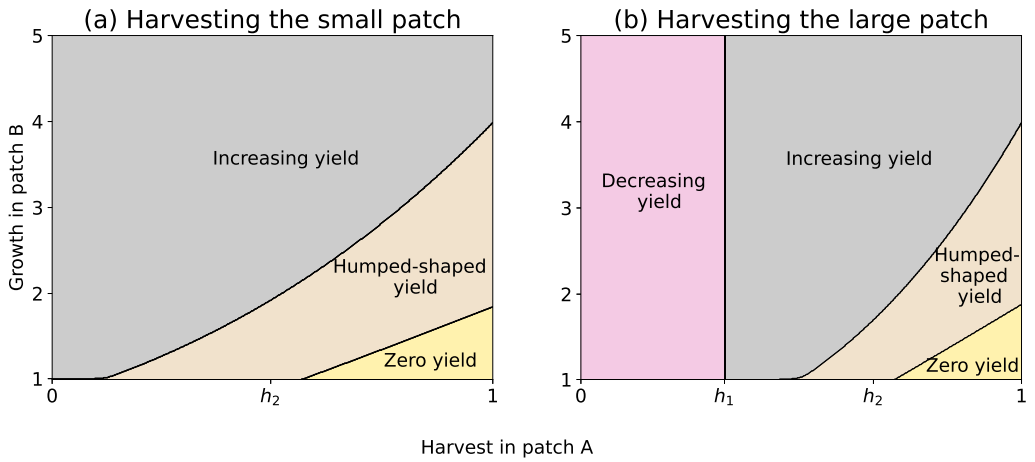

Figure 8: Parameter domains for the four qualitative behaviours of the asymptotic yield to increasing dispersal in discrete time. With (a) Harvesting the small patch (parameter values as in Fig. 5(a)) and (b) Harvesting the large patch (parameter values as in Fig.6(a)). The effective carrying capacity of the harvested patch A becomes equal to the carrying capacity of the protected patch B at h_1 where $K_{\mathrm{B_d}} = \tilde{K}_{\mathrm{A_d}}$. h_2 represents the critical harvesting threshold separating the system in an effective source–source system to the left from an effective source–sink system to the right. This diagram is generated numerically with $K_{\mathrm{A_d}}$ and $K_{\mathrm{B_d}}$ as initial conditions. The asymptotic value of the yield (after 100 time steps) was evaluated for four dispersal values: $\delta_{\mathrm{d}} \in \{0, 0.0001, 0.499, 0.4991\}$ in order to distinguish between the four qualitative behaviours.

is diminished by harvesting to the extent that it is equal to the carrying capacity of the protected patch B, the dynamics resemble those observed when harvesting the initially smaller patch (compare to the ATPS dynamics).

5. Discussion and conclusions

We investigated the impact of increased dispersal between subpopulations, where one population is subjected to proportional harvesting, on the total asymptotic population size (ATPS) and the asymptotic yield. By integrating proportional harvesting into the growth function, we define sustainably harvested dynamics as effective source–source dynamics. In contrast, if overharvesting occurs, the dynamics transitions to effective source–sink dynamics.

We extend previous research on the impacts of increased dispersal on the asymptotic population size in the absence of harvesting, a topic that has received considerable attention in recent years. The source–source environment without harvesting has been fully analysed by [22] in discrete time, who identified four response scenarios and showed that there is a correspondence with the continuous–time results by [20]. The source–sink dynamics without harvesting has been studied in continuous time by [21] and we extended this research by differentiating between the monotonically beneficial and unimodally beneficial response scenarios. In discrete time, [28] observed two of our five response scenarios, namely the beneficial turning detrimental and the extinction response scenarios.

We have completed the categorisation and demonstrated that there exist five response scenarios in the source–sink case with symmetric dispersal. Through a graphical analysis originally introduced by [27] for continuous-time models, we showed that the categorisation in source–sink dynamics of the discrete-time model shows correspondence to those of the continuous-time model with one notable exception: the monotonically detrimental response scenario is absent in continuous time. This discrepancy is attributed to differences between the Beverton–Holt and logistic growth functions. Although these two functions are often considered analogues, their similarity has limitations. The logistic growth function exhibits linear density dependence (which does not accurately reflect the growth patterns of most populations [29]) while the Beverton–Holt function exhibits non-linear density-dependence. A more suitable model, in terms of analogy to the Beverton–Holt growth function

and alignment with real data, might be the theta-logistic growth function which allows convex or concave density dependencies.

When harvesting is introduced into the dynamics of the two-patch model, dispersal is often examined only for specific values, rather than across the entire range. For instance, [30] focused on either isolated or strongly connected patches, and [25] chose three distinct dispersal values. In particular in experiments, it is not feasible to cover a continuous range of dispersal values [23, 24, 26, 25]. Considering that the strength of dispersal can critically determine whether its effect on the ATPS is beneficial or detrimental, we examined the full range of dispersal values while varying harvesting intensity and the growth rate ratios between patches.

Our findings can be distilled into three key statements on how connectivity can affect both ATPS and yield. When comparing the parameter domains of the ATPS key statements with those of the yield in Figure 9, a notable misalignment becomes evident. For example, the "Keep the patches isolated" statement (red) is valid across the entire range for yield when harvesting the larger patch, whereas for the ATPS, it holds true only under conditions of high growth in the protected patch.

1. **The more connectivity the better** (blue area in Fig. 9)
   The only parameter domain where both ATPS and yield monotonically benefit from increased dispersal is when the protected patch is both fast growing and larger, with net migration towards the harvested patch (i.e., when $h \in [h_1, 1]$). In contrast to yield, the ATPS needs stronger growth in the protected patch to sustain the response scenario. Nevertheless, to maintain this response scenario with stronger harvesting, faster growth in the protected area is essential for both yield and ATPS. This is consistent with literature advocating the protection of fast growing patches (i.e., fitness hotspots), to achieve optimal results [31, 13, 32, 11]. If $h \in [0, h_1]$ the blue area of the ATPS indicates a slowly growing and smaller protected patch, with net migration from the harvested patch to the protected patch. The ATPS increases with increasing dispersal, but this comes at the expense of reduced yield, which decreases as dispersal increases.
2. **Medium connectivity is best** (orange area in Fig. 9). If the protected patch is neither a fitness hotspot (high r_{B}) nor growing slowly (low r_{B}), medium connectivity leads to the largest ATPS in the source–source environment ($h \in [0, h_2]$). If the harvested patch becomes a sink

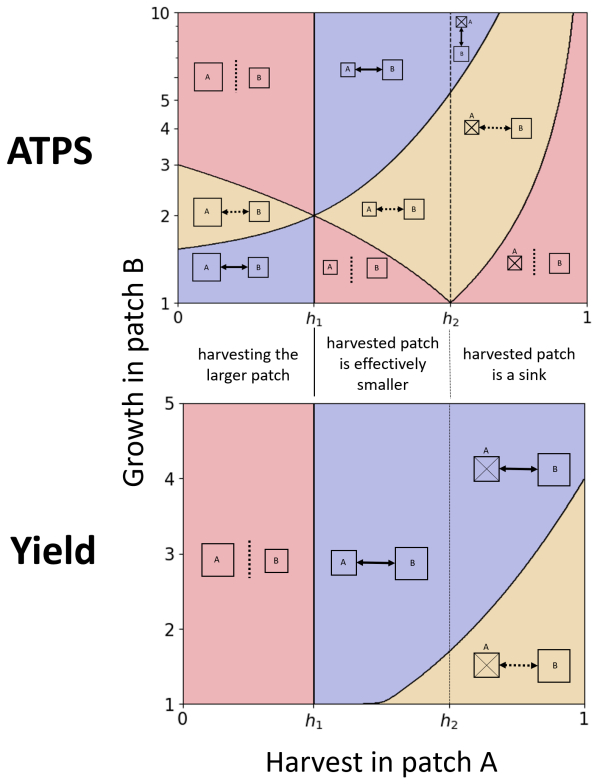

Figure 9: Parameter domains for the qualitative behaviours of the asymptotic total population size (on a logarithmic scale) and asymptotic yield in response to increasing dispersal in discrete time (results are qualitatively similar in continuous time). Patch A is harvested and patch B is protected. The qualitative behaviours are marked by the three sketches and named "The more connectivity the better" (blue, solid arrow), "Medium connectivity is best" (orange, dashed arrow) and "Keep the patches isolated" (red, dashed line). If $h \in [0, h_1]$ the harvested patch A is larger than the protected patch B, if $h \in [h_1, h_2]$ the harvested patch is effectively smaller but acts still as a source and if $h \in [h_2, 1]$ the harvested patch A becomes a sink (box with a cross).

($h \in [h_2, 1]$), medium dispersal is the best option for the ATPS if the growth in the protected patch is also in the medium range.
For yield, medium connectivity is optimal when harvesting is high and the protected patch growth is slow. Low dispersal helps sustain the harvested patch resulting in positive yield. High dispersal places excessive demands on the protected patch's resources, negatively affecting yield: without any remaining ATPS, there will be nothing to harvest.

3. **Keep the patches isolated** (red area in Fig. 9). In the literature, it is well established that the introduction of protected areas can reduce extinction risk [33, 34]. Our findings suggest that total extinction is only possible above a certain dispersal threshold (see Fig. 3(e)): If there is net migration from the protected patch to the harvested patch (i.e., $h \in [h_1, 1]$), strong dispersal with intensive harvesting in one patch can threaten the protected patch's persistence if the harvesting-induced sink is stronger (i.e., negative sink effect). So, in these parameter domains it is best to keep the patches isolated in terms of the ATPS. However, there is no scenario (within $h \in [h_1, 1]$) in which low dispersal decreases yield; particularly when the harvested patch is rescued, yield only becomes positive when the patches are not isolated.
Conversely, when there is net migration from the harvested patch to the protected patch ($h \in [0, h_1]$), it is always optimal to keep the patches isolated in terms of yield, and this is also true for ATPS if the protected patch is fast-growing.

Many studies typically assume a priori that there is unidirectional flow from the protected patch to the harvested patch, commonly referred to as spillover [11, 13]. In contrast, our analysis takes a more general approach by assuming symmetric dispersal. Through this framework, we identified conditions under which the desired spillover does not occur: specifically, when the protected patch is smaller than the harvested patch in terms of effective size. This situation can occur when the harvested patch is subject to low harvesting effort and possesses a larger carrying capacity.

In conclusion, our study offers insights into how different dispersal, harvesting and habitat qualities affect the asymptotic yield and the asymptotic total population size within a two-patch model where one patch is protected and the other one is harvested proportionally. We have discovered that increasing connectivity can serve as a lifeline or a route to extinction, depending on the circumstances: In particular, fast-growing protected patches can res-

cue the harvested patch, while the combination of strong harvesting pressure and/or slowly growing protected populations can lead to the extinction of the total population. Additionally, we found that net migration from the protected patch to the harvested patch is necessary to ensure positive effects on the asymptotic yield. Interestingly, the asymptotic total population size can be positively affected by net migration in both directions. However, if net migration is directed towards the protected patch, the increase of the asymptotic total population size occurs at the cost of reduced yield.

Acknowledgements. The authors acknowledge Daniel Franco for fruitful discussions. FNR would like to express her gratitude for insightful discussions with Friedemann Liebaug, Carolin Grumbach, Jürgen Berlekamp, and Eduardo Liz, as well as extend thanks to the DAAD for facilitating productive research exchanges in Japan and Spain.

Statements and Declarations

Funding

This research was partially supported by the German Academic Exchange Service (DAAD) with funds from the Federal Foreign Office. JS was supported by the Agencia Estatal de Investigación, Spain, and European Regional Development Fund, UE [grant number PID2021-122442NB-I00].

Competing Interests

The authors declare no conflict of interest.

Author Contribution

Formal analysis and investigation of the results: FNR, JS; Methodology: all authors; Conceptualisation and supervision: FMH; Writing - original draft preparation: FNR (lead), JS; Writing- Review and editing: all authors.

ORCID numbers

Femke Naemi Reurik: 0000-0002-1567-4388

Juan Segura: 0000-0002-8314-3458

Frank M. Hilker: 0000-0001-5470-8889

Appendix A. Discrete time

We provide theoretical results for system (1) in the case of effective source–sink dynamics. In what follows, assume $0 < \tilde{r}_{\mathrm{A_d}} \leq 1 < r_{\mathrm{B_d}}$, denote

$\mathbb{R}^2_+ := [0,+\infty) \times [0,+\infty)$ and $\mathbb{R}^2_{++} := (0,+\infty) \times (0,+\infty)$, and define

$$\delta_{\text{crit}_\text{d}} := \frac{(1-\tilde{r}_{\text{A}_\text{d}})(r_{\text{B}_\text{d}}-1)}{\tilde{r}_{\text{A}_\text{d}} + r_{\text{B}_\text{d}} - 2\tilde{r}_{\text{A}_\text{d}} r_{\text{B}_\text{d}}}.$$

The following result shows the conditions for a unique positive equilibrium of system (1).

Proposition 1. *Assume* $0 < \tilde{r}_{\text{A}_\text{d}} \leq 1 < r_{\text{B}_\text{d}}$. *The following holds:*

1. *If* $\delta_\text{d} = 0$, *then* $(0, K_{\text{B}_\text{d}})$ *is a fixed point of system* (1) *such that*

$$\lim_{t\to+\infty} (N_{\text{A}_\text{d}}(t), N_{\text{B}_\text{d}}(t)) = (0, K_{\text{B}_\text{d}})$$

   for any initial condition $(N_{\text{A}_\text{d}}(0), N_{\text{B}_\text{d}}(0)) \in \mathbb{R}^2_+ \setminus \{(0,0)\}$.
2. *If* $\delta_\text{d} \in (0, 0.5]$, $(1-\delta_\text{d})(\tilde{r}_{\text{A}_\text{d}} + r_{\text{B}_\text{d}}) < 2$, $\tilde{r}_{\text{A}_\text{d}} + r_{\text{B}_\text{d}} - 2\tilde{r}_{\text{A}_\text{d}} r_{\text{B}_\text{d}} > 0$, $\tilde{r}_{\text{A}_\text{d}} r_{\text{B}_\text{d}} < 1$, *and* $\delta_\text{d} \geq \delta_{\text{crit}_\text{d}}$, *then the population described by system* (1) *is doomed to extinction, i.e.,*

$$\lim_{t\to+\infty} (N_{\text{A}_\text{d}}(t), N_{\text{B}_\text{d}}(t)) = (0, 0)$$

   for any initial condition $(N_{\text{A}_\text{d}}(0), N_{\text{B}_\text{d}}(0)) \in \mathbb{R}^2_+$.
3. *For all remaining cases, system* (1) *has a fixed point* $(N^*_{\text{A}_\text{d}}, N^*_{\text{B}_\text{d}}) \in \mathbb{R}^2_{++}$ *such that*

$$\lim_{t\to+\infty} (N_{\text{A}_\text{d}}(t), N_{\text{B}_\text{d}}(t)) = (N^*_{\text{A}_\text{d}}, N^*_{\text{B}_\text{d}})$$

   for any initial condition $(N_{\text{A}_\text{d}}(0), N_{\text{B}_\text{d}}(0)) \in \mathbb{R}^2_+ \setminus \{(0,0)\}$.

Proof. For $\delta_\text{d} = 0$, system (1) is an uncoupled system. Since $\tilde{r}_{\text{A}_\text{d}} \leq 1$, all solutions for the first equation of (1) tend to zero, whereas all solutions for the second equation of (1) tend to K_{B_d} given that $r_{B_\text{d}} > 1$. Hence, the first statement follows.

For the second and third statements, following [35], we rewrite system (1) as

$$\begin{pmatrix} N_{\text{A}_\text{d}}(t+1) \\ N_{\text{B}_\text{d}}(t+1) \end{pmatrix} = S_{\delta_\text{d}} \Lambda(N_{\text{A}_\text{d}}(t), N_{\text{B}_\text{d}}(t)) \begin{pmatrix} N_{\text{A}_\text{d}}(t) \\ N_{\text{B}_\text{d}}(t) \end{pmatrix},$$

where

$$S_{\delta_\text{d}} := \begin{pmatrix} 1-\delta_\text{d} & \delta_\text{d} \\ \delta_\text{d} & 1-\delta_\text{d} \end{pmatrix} \quad \text{and} \quad \Lambda(N_{\text{A}_\text{d}}(t), N_{\text{B}_\text{d}}(t)) := \begin{pmatrix} \tilde{f}_{\text{A}_\text{d}} & 0 \\ 0 & f_{\text{B}_\text{d}} \end{pmatrix}.$$

We are going to characterise when the inequality $\rho(S_{\delta_\mathrm{d}}\Lambda(0,0)) > 1$ holds, where $\rho(S_{\delta_\mathrm{d}}\Lambda(0,0))$ denotes the spectral radius of $S_{\delta_\mathrm{d}}\Lambda(0,0)$. Then we will invoke [35, Theorem 2.1] to finish the proof. All elements of the matrix $S_{\delta_\mathrm{d}}\Lambda(0,0)$ are positive, so by the Perron-Frobenius Theorem there exists a simple positive eigenvalue λ such that $\rho(S_{\delta_\mathrm{d}}\Lambda(0,0)) = \lambda$. Therefore, we have that

$$u^2 - 4v > 0 \quad \text{and} \quad \rho(S_{\delta_\mathrm{d}}\Lambda(0,0)) = \frac{u + \sqrt{u^2 - 4v}}{2},$$

where $u = (1-\delta_\mathrm{d})(\tilde{r}_{\mathrm{A_d}} + r_{\mathrm{B_d}})$ and $v = (1-2\delta_\mathrm{d})\tilde{r}_{\mathrm{A_d}} r_{\mathrm{B_d}}$ are the coefficients of the characteristic polynomial of the matrix $S_{\delta_\mathrm{d}}\Lambda(0,0)$. It is straightforward that $\rho(S_{\delta_\mathrm{d}}\Lambda(0,0)) > 1$ if $u \geq 2$.

For the case $u < 2$, we have that

$$\begin{aligned}
\rho(S_{\delta_\mathrm{d}}\Lambda(0,0)) > 1 \;&\Leftrightarrow\; \frac{u + \sqrt{u^2 - 4v}}{2} > 1 \;\Leftrightarrow\; u^2 - 4v > (2-u)^2 \;\Leftrightarrow\; u - v > 1 \\
&\Leftrightarrow\; (1-\delta_\mathrm{d})(\tilde{r}_{\mathrm{A_d}} + r_{\mathrm{B_d}}) - (1-2\delta_\mathrm{d})\tilde{r}_{\mathrm{A_d}} r_{\mathrm{B_d}} > 1 \\
&\Leftrightarrow\; \tilde{r}_{\mathrm{A_d}} + r_{\mathrm{B_d}} - \tilde{r}_{\mathrm{A_d}} r_{\mathrm{B_d}} - 1 > \delta_\mathrm{d}(\tilde{r}_{\mathrm{A_d}} + r_{\mathrm{B_d}} - 2\tilde{r}_{\mathrm{A_d}} r_{\mathrm{B_d}}) \\
&\Leftrightarrow\; (r_{\mathrm{B_d}} - 1)(1 - \tilde{r}_{\mathrm{A_d}}) > \delta_\mathrm{d}(\tilde{r}_{\mathrm{A_d}} + r_{\mathrm{B_d}} - 2\tilde{r}_{\mathrm{A_d}} r_{\mathrm{B_d}}). \quad \text{(A.1)}
\end{aligned}$$

Assume $\tilde{r}_{\mathrm{A_d}} \neq 1$ and $\tilde{r}_{\mathrm{A_d}} + r_{\mathrm{B_d}} - 2\tilde{r}_{\mathrm{A_d}} r_{\mathrm{B_d}} > 0$. We distinguish two subcases. If $\tilde{r}_{\mathrm{A_d}} r_{\mathrm{B_d}} \geq 1$, then condition (A.1) holds:

$$\begin{aligned}
(r_{\mathrm{B_d}} - 1)(1 - \tilde{r}_{\mathrm{A_d}}) &= \tilde{r}_{\mathrm{A_d}} + r_{\mathrm{B_d}} - \tilde{r}_{\mathrm{A_d}} r_{\mathrm{B_d}} - 1 \\
&= \tilde{r}_{\mathrm{A_d}} + r_{\mathrm{B_d}} - 2\tilde{r}_{\mathrm{A_d}} r_{\mathrm{B_d}} + \tilde{r}_{\mathrm{A_d}} r_{\mathrm{B_d}} - 1 \\
&\geq \tilde{r}_{\mathrm{A_d}} + r_{\mathrm{B_d}} - 2\tilde{r}_{\mathrm{A_d}} r_{\mathrm{B_d}} \\
&> \delta_\mathrm{d}(\tilde{r}_{\mathrm{A_d}} + r_{\mathrm{B_d}} - 2\tilde{r}_{\mathrm{A_d}} r_{\mathrm{B_d}}).
\end{aligned}$$

If $\tilde{r}_{\mathrm{A_d}} r_{\mathrm{B_d}} < 1$, then it is straightforward that condition (A.1) holds if and only if $\delta_\mathrm{d} < \delta_{\mathrm{crit_d}}$.

Finally, for the cases $\tilde{r}_{\mathrm{A_d}} = 1$ or $\tilde{r}_{\mathrm{A_d}} + r_{\mathrm{B_d}} - 2\tilde{r}_{\mathrm{A_d}} r_{\mathrm{B_d}} \leq 0$, condition (A.1) is trivially met. Note that these two cases cannot occur simultaneously. For the first case, $\tilde{r}_{\mathrm{A_d}} r_{\mathrm{B_d}} = r_{\mathrm{B_d}} > 1$. For the second case, it is routine to check that the infimum of the function xy subject to the constraints $0 < x \leq 1 < y$ and $x + y - 2xy \leq 0$ equals 1 and is obtained for $x = 1$ and $y \to 1$. Hence, $\tilde{r}_{\mathrm{A_d}} + r_{\mathrm{B_d}} - 2\tilde{r}_{\mathrm{A_d}} r_{\mathrm{B_d}} \leq 0$ implies $\tilde{r}_{\mathrm{A_d}} r_{\mathrm{B_d}} > 1$. This completes the proof, and the statement follows from [35, Theorem 2.1]. □

Corollary 1. *Assume* $0 < \tilde{r}_{A_\mathrm{d}} \leq 1 < r_{B_\mathrm{d}}$. *The population described by system* (1) *goes extinct in the long run if and only if* $\tilde{r}_{\mathrm{A_d}} + r_{\mathrm{B_d}} \leq 2$ *and* $\delta_\mathrm{d} \geq \delta_{\mathrm{crit_d}}$.

Proof. By Proposition 1, the population goes extinct if and only if $(1 - \delta_\mathrm{d})(\tilde{r}_{\mathrm{A_d}} + r_{\mathrm{B_d}}) < 2$, $\tilde{r}_{\mathrm{A_d}} + r_{\mathrm{B_d}} - 2\tilde{r}_{\mathrm{A_d}} r_{\mathrm{B_d}} > 0$, $\tilde{r}_{\mathrm{A_d}} r_{\mathrm{B_d}} < 1$, and $\delta_\mathrm{d} \geq \delta_{\mathrm{crit_d}}$. From the latter condition, it must be $\delta_{\mathrm{crit_d}} \leq 0.5$, which is equivalent to $\tilde{r}_{\mathrm{A_d}} + r_{\mathrm{B_d}} \leq 2$. In particular, this implies $(1 - \delta_\mathrm{d})(\tilde{r}_{\mathrm{A_d}} + r_{\mathrm{B_d}}) < 2$. Moreover, it is routine to check that the infimum of the function $x + y - 2xy$ and the supremum of the function xy under the constraints $0 < x \leq 1 < y$ and $x + y \leq 2$ are 0 and 1, respectively, and the two of them are obtained for $x = 1$ and $y \to 1$. Hence, the condition $\tilde{r}_{\mathrm{A_d}} + r_{\mathrm{B_d}} \leq 2$ also guarantees $\tilde{r}_{\mathrm{A_d}} + r_{\mathrm{B_d}} - 2\tilde{r}_{\mathrm{A_d}} r_{\mathrm{B_d}} > 0$ and $\tilde{r}_{\mathrm{A_d}} r_{\mathrm{B_d}} < 1$, and the statement follows. □

In what follows, when it exists, we make explicit the dependence of the fixed point of system (1) on the dispersal rate, by writing this point in the form $(N^*_{\mathrm{A_d}}(\delta_\mathrm{d}), N^*_{\mathrm{B_d}}(\delta_\mathrm{d}))$. By Corollary 1, the function $H\colon D \to \mathbb{R}$ given by

$$H(\delta_\mathrm{d}) := N^*_{\mathrm{A_d}}(\delta_\mathrm{d}) + N^*_{\mathrm{B_d}}(\delta_\mathrm{d}) - K_{\mathrm{B_d}},$$

where

$$D = \begin{cases} [0, 0.5] & \text{if} \quad \tilde{r}_{\mathrm{A_d}} + r_{\mathrm{B_d}} > 2, \\ [0, \delta_{\mathrm{crit_d}}) & \text{if} \quad \tilde{r}_{\mathrm{A_d}} + r_{\mathrm{B_d}} \leq 2, \end{cases}$$

is well defined. In what follows, $\mathring{D}$ will denote the interior of D. Clearly, H vanishes at $\delta_\mathrm{d} = 0$. The following results show that H can have at most another zero given by the expression

$$\delta^\dagger_\mathrm{d} := \frac{\tilde{K}_{\mathrm{A_d}}(\tilde{K}_{\mathrm{A_d}} - K_{\mathrm{B_d}})(1 - \tilde{r}_{\mathrm{A_d}})(r_{\mathrm{B_d}} - 1)(\tilde{r}_{\mathrm{A_d}} r_{\mathrm{B_d}} - 1)}{P}, \tag{A.2}$$

with

$$P := (\tilde{K}_{\mathrm{A_d}} \tilde{r}_{\mathrm{A_d}}(r_{\mathrm{B_d}} - 1) - K_{\mathrm{B_d}}(1 - \tilde{r}_{\mathrm{A_d}}))(\tilde{K}_{\mathrm{A_d}}(1 + r_{\mathrm{B_d}} - 2\tilde{r}_{\mathrm{A_d}} r_{\mathrm{B_d}}) - K_{\mathrm{B_d}}(1 - \tilde{r}_{\mathrm{A_d}}) r_{\mathrm{B_d}}).$$

Proposition 2. *Assume* $0 < \tilde{r}_{\mathrm{A_d}} \leq 1 < r_{\mathrm{B_d}}$. *If* $P = 0$ *or* $\delta^\dagger_\mathrm{d} \notin D$, *then* H *has a unique zero,* $\delta_\mathrm{d} = 0$. *Otherwise,* H *has two zeros, which are* $\delta_\mathrm{d} = 0$ *and* $\delta_\mathrm{d} = \delta^\dagger_\mathrm{d}$.

Proof. Assume $H(\delta_{\mathrm{d}}) = 0$ for $\delta_{\mathrm{d}} \in [0, 0.5]$. We have that $N^*_{\mathrm{A_d}}(\delta_{\mathrm{d}})$ and $N^*_{\mathrm{B_d}}(\delta_{\mathrm{d}})$ are given by the system of equations

$$\begin{cases} N^*_{\mathrm{A_d}}(\delta_{\mathrm{d}}) = (1-\delta_{\mathrm{d}})\tilde{f}_{\mathrm{A_d}}(N^*_{\mathrm{A_d}}(\delta_{\mathrm{d}})) + \delta_{\mathrm{d}} f_{\mathrm{B_d}}(N^*_{\mathrm{B_d}}(\delta_{\mathrm{d}})), \\ N^*_{\mathrm{B_d}}(\delta_{\mathrm{d}}) = \delta_{\mathrm{d}}\tilde{f}_{\mathrm{A_d}}(N^*_{\mathrm{A_d}}(\delta_{\mathrm{d}})) + (1-\delta_{\mathrm{d}}) f_{\mathrm{B_d}}(N^*_{\mathrm{B_d}}(\delta_{\mathrm{d}})), \end{cases} \tag{A.3}$$

and by adding these equations we obtain

$$N^*_{\mathrm{A_d}}(\delta_{\mathrm{d}}) + N^*_{\mathrm{B_d}}(\delta_{\mathrm{d}}) = \tilde{f}_{\mathrm{A_d}}(N^*_{\mathrm{A_d}}(\delta_{\mathrm{d}})) + f_{\mathrm{B_d}}(N^*_{\mathrm{B_d}}(\delta_{\mathrm{d}})).$$

From the assumption $H(\delta_{\mathrm{d}}) = 0$, we obtain

$$N^*_{\mathrm{A_d}}(\delta_{\mathrm{d}}) + N^*_{\mathrm{B_d}}(\delta_{\mathrm{d}}) = K_{\mathrm{B_d}}. \tag{A.4}$$

Therefore, $N^*_{\mathrm{A_d}}(\delta_{\mathrm{d}})$ and $N^*_{\mathrm{B_d}}(\delta_{\mathrm{d}})$ are solutions of the system

$$\begin{cases} N^*_{\mathrm{A_d}}(\delta_{\mathrm{d}}) + N^*_{\mathrm{B_d}}(\delta_{\mathrm{d}}) = \tilde{f}_{\mathrm{A_d}}(N^*_{\mathrm{A_d}}(\delta_{\mathrm{d}})) + f_{\mathrm{B_d}}(N^*_{\mathrm{B_d}}(\delta_{\mathrm{d}})), \\ N^*_{\mathrm{A_d}}(\delta_{\mathrm{d}}) + N^*_{\mathrm{B_d}}(\delta_{\mathrm{d}}) = K_{\mathrm{B_d}}. \end{cases} \tag{A.5}$$

System (A.5) has at most two solutions, which are

$$(N^*_{\mathrm{A_d}}(\delta_{\mathrm{d}}), N^*_{\mathrm{B_d}}(\delta_{\mathrm{d}})) = (0, K_{\mathrm{B_d}}) \qquad \text{and}$$
$$(N^*_{\mathrm{A_d}}(\delta_{\mathrm{d}}), N^*_{\mathrm{B_d}}(\delta_{\mathrm{d}})) = \left(\frac{\tilde{K}_{\mathrm{A_d}} K_{\mathrm{B_d}} (\tilde{r}_{\mathrm{A_d}} r_{\mathrm{B_d}} - 1)}{Q}, \frac{K_{\mathrm{B_d}} (\tilde{K}_{\mathrm{A_d}} - K_{\mathrm{B_d}})(1 - \tilde{r}_{\mathrm{A_d}})}{Q} \right),$$

where $Q = \tilde{K}_{\mathrm{A_d}} \tilde{r}_{\mathrm{A_d}} (r_{\mathrm{B_d}} - 1) - K_{\mathrm{B_d}} (1 - \tilde{r}_{\mathrm{A_d}})$. Moreover, from the first equation of (A.3) and system (A.5), we obtain

$$(K_{\mathrm{B_d}} - 2\tilde{f}_{\mathrm{A_d}}(N^*_{\mathrm{A_d}}(\delta_{\mathrm{d}})))\delta_{\mathrm{d}} = N^*_{\mathrm{A_d}}(\delta_{\mathrm{d}}) - \tilde{f}_{\mathrm{A_d}}(N^*_{\mathrm{A_d}}(\delta_{\mathrm{d}})).$$

If we substitute $N^*_{\mathrm{A_d}}(\delta_{\mathrm{d}}) = 0$ into the previous equality, we obtain $\delta_{\mathrm{d}} = 0$, and if we substitute $N^*_{\mathrm{A_d}}(\delta_{\mathrm{d}}) = \frac{\tilde{K}_{\mathrm{A_d}} K_{\mathrm{B_d}} (\tilde{r}_{\mathrm{A_d}} r_{\mathrm{B_d}} - 1)}{Q}$, we obtain

$$P\delta_{\mathrm{d}} = \tilde{K}_{\mathrm{A_d}} (\tilde{K}_{\mathrm{A_d}} - K_{\mathrm{B_d}})(1 - \tilde{r}_{\mathrm{A_d}})(r_{\mathrm{B_d}} - 1)(\tilde{r}_{\mathrm{A_d}} r_{\mathrm{B_d}} - 1).$$

If $P = 0$, the previous equality is inconsistent and thus $\delta_{\mathrm{d}} = 0$ is the unique zero of H. Otherwise, we obtain $\delta_{\mathrm{d}} = \delta^\dagger_{\mathrm{d}}$, which is another zero of H if $\delta^\dagger_{\mathrm{d}} \in D$. □

The situation described in Proposition 2 can be observed in Fig. 3. Panel (c) corresponds to the cases in which $P \neq 0$ and $\delta_{\mathrm{d}}^{\dagger} \in D$, for which the graph crosses the horizontal line ATPS_0 at the abscissa $\delta_{\mathrm{d}}^{\dagger}$. The remaining panels correspond to situations in which either $P = 0$ or $\delta_{\mathrm{d}}^{\dagger} \notin D$, for which the graph is always either above or below ATPS_0.

Next, we calculate the derivative $H'(0^+)$.

Proposition 3. *Assume* $0 < \tilde{r}_{\mathrm{A_d}} < 1 < r_{\mathrm{B_d}}$. *Then,*

$$H'(0^+) = \frac{(\tilde{r}_{\mathrm{A_d}} r_{\mathrm{B_d}} - 1)K_{\mathrm{B_d}}}{(1 - \tilde{r}_{\mathrm{A_d}})(r_{\mathrm{B_d}} - 1)}.$$

Proof. We recall that $N^*_{\mathrm{A_d}}(\delta_{\mathrm{d}})$ and $N^*_{\mathrm{B_d}}(\delta_{\mathrm{d}})$ are implicitly defined by system (A.3). Consider the function $F\colon \mathbb{R}^3 \to \mathbb{R}^2$ given by $F(\delta_{\mathrm{d}}, \bar{N}_{\mathrm{A}}, \bar{N}_{\mathrm{B}}) = (F_1(\delta_{\mathrm{d}}, \bar{N}_{\mathrm{A}}, \bar{N}_{\mathrm{B}}), F_2(\delta_{\mathrm{d}}, \bar{N}_{\mathrm{A}}, \bar{N}_{\mathrm{B}}))$, with

$$\begin{aligned} F_1(\delta_{\mathrm{d}}, \bar{N}_{\mathrm{A}}, \bar{N}_{\mathrm{B}}) &= (1 - \delta_{\mathrm{d}})\tilde{f}_{\mathrm{A_d}}(\bar{N}_{\mathrm{A}}) + \delta_{\mathrm{d}} f_{\mathrm{B_d}}(\bar{N}_{\mathrm{B}}) - \bar{N}_{\mathrm{A}}, \\ F_2(\delta_{\mathrm{d}}, \bar{N}_{\mathrm{A}}, \bar{N}_{\mathrm{B}}) &= \delta_{\mathrm{d}}\tilde{f}_{\mathrm{A_d}}(\bar{N}_{\mathrm{A}}) + (1 - \delta_{\mathrm{d}}) f_{\mathrm{B_d}}(\bar{N}_{\mathrm{B}}) - \bar{N}_{\mathrm{B}}. \end{aligned}$$

To prove that $(N^*_{\mathrm{A_d}})'(0^+)$ and $(N^*_{\mathrm{B_d}})'(0^+)$ are finite, we apply the Implicit Function Theorem to the system $F(\delta_{\mathrm{d}}, \bar{N}_{\mathrm{A}}, \bar{N}_{\mathrm{B}}) = (0, 0)$ around the point $(0, N^*_{\mathrm{A_d}}(0), N^*_{\mathrm{B_d}}(0)) = (0, 0, K_{\mathrm{B_d}})$. Since $f'_{\mathrm{A_d}}(0) = \tilde{r}_{\mathrm{A_d}}$ and $f'_{\mathrm{B_d}}(K_{\mathrm{B_d}}) = \frac{1}{r_{\mathrm{B}}}$, we have that

$$\left.\begin{vmatrix} \frac{\partial F_1}{\partial \bar{N}_{\mathrm{A}}} & \frac{\partial F_1}{\partial \bar{N}_{\mathrm{B}}} \\ \frac{\partial F_2}{\partial \bar{N}_{\mathrm{A}}} & \frac{\partial F_2}{\partial \bar{N}_{\mathrm{B}}} \end{vmatrix}\right|_{|(0,0,K_{\mathrm{B_d}})} = \begin{vmatrix} \tilde{r}_{\mathrm{A_d}} - 1 & 0 \\ 0 & \frac{1 - r_{\mathrm{B}}}{r_{\mathrm{B}}} \end{vmatrix} \neq 0.$$

This proves that there exists $\zeta > 0$ such that the system $F(\delta_{\mathrm{d}}, \bar{N}_{\mathrm{A}}, \bar{N}_{\mathrm{B}}) = (0, 0)$ defines two differentiable functions $\bar{N}_{\mathrm{A}}(\delta_{\mathrm{d}})$ and $\bar{N}_{\mathrm{B}}(\delta_{\mathrm{d}})$ for $\delta_{\mathrm{d}} \in (-\zeta, \zeta)$. Clearly, if $\delta_{\mathrm{d}} \in [0, \zeta)$, the point $(\bar{N}_{\mathrm{A}}(\delta_{\mathrm{d}}), \bar{N}_{\mathrm{B}}(\delta_{\mathrm{d}}))$ is a fixed point of system (1). By Proposition 1, we conclude that $\bar{N}_{\mathrm{A}}(\delta_{\mathrm{d}}) = N^*_{\mathrm{A_d}}(\delta_{\mathrm{d}})$ and $\bar{N}_{\mathrm{B}}(\delta_{\mathrm{d}}) = N^*_{\mathrm{B_d}}(\delta_{\mathrm{d}})$ for $\delta_{\mathrm{d}} \in [0, \zeta)$, which proves that $(N^*_{\mathrm{A_d}})'(0^+) = \bar{N}'_{\mathrm{A}}(0)$ and $(N^*_{\mathrm{B_d}})'(0^+) = \bar{N}'_{\mathrm{B}}(0)$ are finite.

By differentiating with respect to δ_{d} in system (A.3) and taking $\delta_{\mathrm{d}} \to 0^+$ we arrive at

$$\begin{cases} (N^*_{\mathrm{A_d}})'(0^+) = -\tilde{f}_{\mathrm{A_d}}(N^*_{\mathrm{A_d}}(0)) + f'_{\mathrm{A_d}}(N^*_{\mathrm{A_d}}(0))(N^*_{\mathrm{A_d}})'(0^+) + f_{\mathrm{B_d}}(N^*_{\mathrm{B_d}}(0)), \\ (N^*_{\mathrm{B_d}})'(0^+) = \tilde{f}_{\mathrm{A_d}}(N^*_{\mathrm{A_d}}(0)) - f_{\mathrm{B_d}}(N^*_{\mathrm{B_d}}(0)) + f'_{\mathrm{B_d}}(N^*_{\mathrm{B_d}}(0))(N^*_{\mathrm{B_d}})'(0^+). \end{cases}$$

Since $\tilde{f}_{\mathrm{A_d}}(N^*_{\mathrm{A_d}}(0)) = 0$, $f_{\mathrm{B_d}}(N^*_{\mathrm{B_d}}(0)) = K_{\mathrm{B_d}}$, $\tilde{f}'_{\mathrm{A_d}}(N^*_{\mathrm{A_d}}(0)) = \tilde{r}_{\mathrm{A_d}}$, and $f'_{\mathrm{B_d}}(N^*_{\mathrm{B_d}}(0)) = \frac{1}{r_{\mathrm{B_d}}}$, we obtain

$$\begin{cases} (N^*_{\mathrm{A_d}})'(0^+) = \frac{K_{\mathrm{B_d}}}{1-\tilde{r}_{\mathrm{A_d}}}, \\ (N^*_{\mathrm{B_d}})'(0^+) = -\frac{r_{\mathrm{B_d}} K_{\mathrm{B_d}}}{r_{\mathrm{B_d}}-1}. \end{cases}$$

Thus,

$$H'(0^+) = (N^*_{\mathrm{A_d}})'(0^+) + (N^*_{\mathrm{B_d}})'(0^+) = \frac{(\tilde{r}_{\mathrm{A_d}} r_{\mathrm{B_d}} - 1)K_{\mathrm{B_d}}}{(1-\tilde{r}_{\mathrm{A_d}})(r_{\mathrm{B_d}}-1)}.$$

□

Now, we study how H varies with the dispersal rate. Define

$$\begin{aligned} A &\coloneqq (\tilde{K}_{\mathrm{A_d}}\sqrt{\tilde{r}_{\mathrm{A_d}}}(r_{\mathrm{B_d}}-1) + K_{\mathrm{B_d}}(\tilde{r}_{\mathrm{A_d}}-1)\sqrt{r_{\mathrm{B_d}}})(r_{\mathrm{B_d}}-1), \\ B &\coloneqq K_{\mathrm{B_d}}(2\tilde{K}_{\mathrm{A_d}}\sqrt{\tilde{r}_{\mathrm{A_d}}} - (\tilde{K}_{\mathrm{A_d}} - K_{\mathrm{B_d}} + (\tilde{K}_{\mathrm{A_d}} + K_{\mathrm{B_d}})\tilde{r}_{\mathrm{A_d}})\sqrt{r_{\mathrm{B_d}}})(r_{\mathrm{B_d}}-1), \\ C &\coloneqq \tilde{K}_{\mathrm{A_d}} K^2_{\mathrm{B_d}}(\sqrt{\tilde{r}_{\mathrm{A_d}}} - (1+\tilde{r}_{\mathrm{A_d}})\sqrt{r_{\mathrm{B_d}}} + \sqrt{\tilde{r}_{\mathrm{A_d}}} r_{\mathrm{B_d}}). \end{aligned}$$

Lemma 1. *Assume $0 < \tilde{r}_{\mathrm{A_d}} < 1 < r_{\mathrm{B_d}}$. Then, the equation $Ax^2+Bx+C = 0$ has two simple real roots.*

Proof. To simplify the calculations, we define $\tilde{M}_{\mathrm{A_d}} \coloneqq \tilde{K}_{\mathrm{A_d}}/(\tilde{r}_{\mathrm{A_d}} - 1)$ and $M_{\mathrm{B_d}} \coloneqq K_{\mathrm{B_d}}/(r_{\mathrm{B_d}} - 1)$. It is straightforward that $\tilde{M}_{\mathrm{A_d}} > 0$ and $M_{\mathrm{B_d}} > 0$. Consider the terms

$$\begin{aligned} a &\coloneqq \frac{A}{(\tilde{r}_{\mathrm{A_d}}-1)^2(r_{\mathrm{B_d}}-1)} = \tilde{M}_{\mathrm{A_d}}\sqrt{\tilde{r}_{\mathrm{A_d}}} + M_{\mathrm{B_d}}\sqrt{r_{\mathrm{B_d}}}, \\ b &\coloneqq \frac{B}{(\tilde{r}_{\mathrm{A_d}}-1)^2(r_{\mathrm{B_d}}-1)} \\ &= \tilde{M}^2_{\mathrm{A_d}}\sqrt{\tilde{r}_{\mathrm{A_d}}}(1-\tilde{r}_{\mathrm{A_d}}) + \tilde{M}_{\mathrm{A_d}} M_{\mathrm{B_d}}\left(\sqrt{r_{\mathrm{B_d}}} - \sqrt{\tilde{r}_{\mathrm{A_d}}} + \sqrt{r_{\mathrm{B_d}}}(1-\sqrt{\tilde{r}_{\mathrm{A_d}} r_{\mathrm{B_d}}})\right), \\ c &\coloneqq \frac{C}{(\tilde{r}_{\mathrm{A_d}}-1)^2(r_{\mathrm{B_d}}-1)} = \tilde{M}^2_{\mathrm{A_d}} M_{\mathrm{B_d}}(\sqrt{\tilde{r}_{\mathrm{A_d}}} - \sqrt{r_{\mathrm{B_d}}})(\sqrt{\tilde{r}_{\mathrm{A_d}} r_{\mathrm{B_d}}} - 1). \end{aligned}$$

The result follows from the fact that the discriminant of the equation $ax^2 + bx + c = 0$ is positive,

$$\begin{aligned} b^2 - 4ac = \tilde{M}^2_{\mathrm{A_d}}\tilde{r}_{\mathrm{A_d}}(&\tilde{M}^2_{\mathrm{A_d}}(\tilde{r}_{\mathrm{A_d}}-1)^2 + M^2_{\mathrm{B_d}}(r_{\mathrm{B_d}}-1)^2 \\ &+ 2\tilde{M}_{\mathrm{A_d}} M_{\mathrm{B_d}}((\sqrt{\tilde{r}_{\mathrm{A_d}}} - \sqrt{r_{\mathrm{B_d}}})^2 + (\sqrt{\tilde{r}_{\mathrm{A_d}} r_{\mathrm{B_d}}} - 1)^2)). \end{aligned}$$

□

By using Lemma 1, denote by x^* the largest root of the equation $Ax^2 + Bx + C = 0$, and define

$$y^* \coloneqq \frac{K_{\mathrm{B_d}}(\tilde{K}_{\mathrm{A_d}}(\sqrt{r_{\mathrm{B_d}}} - \sqrt{\tilde{r}_{\mathrm{A_d}}}) + (\tilde{r}_{\mathrm{A_d}} - 1)\sqrt{r_{\mathrm{B_d}}}x^*)}{\tilde{K}_{\mathrm{A_d}}\sqrt{\tilde{r}_{\mathrm{A_d}}}(r_{\mathrm{B_d}} - 1)}.$$

Proposition 4. *Assume* $0 < \tilde{r}_{\mathrm{A_d}} < 1 < r_{\mathrm{B_d}}$. *Then,* $\tilde{f}_{\mathrm{A_d}}(x^*) \neq f_{\mathrm{B_d}}(y^*)$, *and if we define*

$$\delta_{\max_{\mathrm{d}}} \coloneqq \frac{y^* - f_{\mathrm{B_d}}(y^*)}{\tilde{f}_{\mathrm{A_d}}(x^*) - f_{\mathrm{B_d}}(y^*)},$$

then the following holds:

1. *If* $\delta_{\max_{\mathrm{d}}} \notin \mathring{D}$, *then* H *is strictly monotonic in* D.
2. *If* $\delta_{\max_{\mathrm{d}}} \in \mathring{D}$, *then* H *is strictly increasing in* $[0, \delta_{\max_{\mathrm{d}}})$ *and strictly decreasing in* $D \setminus [0, \delta_{\max_{\mathrm{d}}})$.

Proof. Assume that $H'(\delta_{\mathrm{d}}) = 0$ for $\delta_{\mathrm{d}} \in \mathring{D}$. From the expression of H, this is equivalent to $(N^*_{\mathrm{A_d}})'(\delta_{\mathrm{d}}) + (N^*_{\mathrm{B_d}})'(\delta_{\mathrm{d}}) = 0$. By adding the two equations in system (A.3) and differentiating with respect to δ_{d}, we obtain

$$(N^*_{\mathrm{A_d}})'(\delta_{\mathrm{d}}) + (N^*_{\mathrm{B_d}})'(\delta_{\mathrm{d}}) = f'_{\mathrm{A_d}}(N^*_{\mathrm{A_d}}(\delta_{\mathrm{d}}))(N^*_{\mathrm{A_d}})'(\delta_{\mathrm{d}}) + f'_{\mathrm{B_d}}(N^*_{\mathrm{B_d}}(\delta_{\mathrm{d}}))(N^*_{\mathrm{B_d}})'(\delta_{\mathrm{d}}), \tag{A.6}$$

which after substituting $(N^*_{\mathrm{B_d}})'(\delta_{\mathrm{d}}) = -(N^*_{\mathrm{A_d}})'(\delta_{\mathrm{d}})$ leads to

$$(f'_{\mathrm{A_d}}(N^*_{\mathrm{A_d}}(\delta_{\mathrm{d}})) - f'_{\mathrm{B_d}}(N^*_{\mathrm{B_d}}(\delta_{\mathrm{d}}))) \cdot (N^*_{\mathrm{A_d}})'(\delta_{\mathrm{d}}) = 0.$$

Suppose $(N^*_{\mathrm{A_d}})'(\delta_{\mathrm{d}}) = 0$. Then, $(N^*_{\mathrm{B_d}})'(\delta_{\mathrm{d}}) = 0$. Substitution into the system obtained from differentiating (A.3) with respect to δ_{d} gives $\tilde{f}_{\mathrm{A_d}}(N^*_{\mathrm{A_d}}(\delta_{\mathrm{d}})) = f_{\mathrm{B_d}}(N^*_{\mathrm{B_d}}(\delta_{\mathrm{d}}))$. If we impose this condition, then system (A.3) reads

$$\begin{cases} N^*_{\mathrm{A_d}}(\delta_{\mathrm{d}}) = \tilde{f}_{\mathrm{A_d}}(N^*_{\mathrm{A_d}}(\delta_{\mathrm{d}})), \\ N^*_{\mathrm{B_d}}(\delta_{\mathrm{d}}) = f_{\mathrm{B_d}}(N^*_{\mathrm{B_d}}(\delta_{\mathrm{d}})), \end{cases}$$

and therefore $N^*_{\mathrm{A_d}}(\delta_{\mathrm{d}}) = 0$ and $N^*_{\mathrm{B_d}}(\delta_{\mathrm{d}}) = K_{\mathrm{B_d}}$. The latter is absurd because, by Proposition 1, necessarily $\delta_{\mathrm{d}} = 0$, and we are seeking stationary points of H in the interior of its domain. Hence, $f'_{\mathrm{A_d}}(N^*_{\mathrm{A_d}}(\delta_{\mathrm{d}})) = f'_{\mathrm{B_d}}(N^*_{\mathrm{B_d}}(\delta_{\mathrm{d}}))$, which is equivalent to

$$N^*_{\mathrm{B_d}}(\delta_{\mathrm{d}}) = \frac{K_{\mathrm{B_d}}(\tilde{K}_{\mathrm{A_d}}(\sqrt{r_{\mathrm{B_d}}} - \sqrt{\tilde{r}_{\mathrm{A_d}}}) + (\tilde{r}_{\mathrm{A_d}} - 1)\sqrt{r_{\mathrm{B_d}}}N^*_{\mathrm{A_d}}(\delta_{\mathrm{d}}))}{\tilde{K}_{\mathrm{A_d}}\sqrt{\tilde{r}_{\mathrm{A_d}}}(r_{\mathrm{B_d}} - 1)}. \tag{A.7}$$

The sum of the equations in (A.3) yields

$$N^*_{\mathrm{A_d}}(\delta_\mathrm{d}) + N^*_{\mathrm{B_d}}(\delta_\mathrm{d}) = \tilde{f}_{\mathrm{A_d}}(N^*_{\mathrm{A_d}}(\delta_\mathrm{d})) + f_{\mathrm{B_d}}(N^*_{\mathrm{B_d}}(\delta_\mathrm{d})),$$

which is equivalent to

$$A(N^*_{\mathrm{A_d}}(\delta_\mathrm{d}))^2 + BN^*_{\mathrm{A_d}}(\delta_\mathrm{d}) + C = 0 \tag{A.8}$$

after substituting the value of $N^*_{\mathrm{B_d}}(\delta_\mathrm{d})$ in (A.7). Hence, $N^*_{\mathrm{A_d}}(\delta_\mathrm{d})$ is one of the roots stated in Lemma 1. We now distinguish three cases.

(a) Assume $\tilde{r}_{\mathrm{A_d}} r_{\mathrm{B_d}} < 1$. In this case, under the assumptions in the statement, A, B and C are positive, and thus the two roots of the equation $Ax^2 + Bx + C = 0$ are negative. Hence, H has no stationary points in the interior of its domain.

(b) Assume $\tilde{r}_{\mathrm{A_d}} r_{\mathrm{B_d}} = 1$. In this case, under the assumptions in the statement, $A > 0$, $B > 0$ and $C = 0$, and thus the two roots of Ax^2+Bx+C are $-B/A < 0$ and 0. Hence, $N^*_{\mathrm{A_d}}(\delta_\mathrm{d}) = 0$, and by Proposition 1 necessarily $\delta_\mathrm{d} = 0$. This proves that in this case H neither has stationary points in the interior of its domain.

(c) Assume $\tilde{r}_{\mathrm{A_d}} r_{\mathrm{B_d}} > 1$. Under the assumptions in the statement, $A > 0$ and $C < 0$, and therefore the two roots of $Ax^2 + Bx + C = 0$ are nonzero and have different signs. This implies $N^*_{\mathrm{A_d}}(\delta_\mathrm{d}) = x^* > 0$. Notice that, under the assumptions in the statement, $y^* > 0$ if $x^* > 0$. This, together with equation (A.7), yields $N^*_{\mathrm{B_d}}(\delta_\mathrm{d}) = y^* > 0$. Moreover, we have seen that necessarily $f_A(x^*) \neq f_B(y^*)$, and thus $\delta_{\max_\mathrm{d}}$ is well defined. For all the above, H has stationary points in the interior of its domain if and only if

$$(N^*_{\mathrm{A_d}}(\delta_\mathrm{d}), N^*_{\mathrm{B_d}}(\delta_\mathrm{d})) = (x^*, y^*)$$

for some $\delta_\mathrm{d} \in \mathring{D}$. This is equivalent to say that (x^*, y^*) satisfies system (A.3) for some $\delta_\mathrm{d} \in \mathring{D}$, i.e.,

$$\begin{cases} x^* = (1-\delta_\mathrm{d})\tilde{f}_{\mathrm{A_d}}(x^*) + \delta_\mathrm{d} f_{\mathrm{B_d}}(y^*), \\ y^* = \delta_\mathrm{d}\tilde{f}_{\mathrm{A_d}}(x^*) + (1-\delta_\mathrm{d}) f_{\mathrm{B_d}}(y^*). \end{cases} \tag{A.9}$$

The sum of these two equalities is

$$x^* + y^* = \tilde{f}_{\mathrm{A_d}}(x^*) + f_{\mathrm{B_d}}(y^*),$$

which is met by the construction done above. Hence, it is enough to impose any of the two equalities in (A.9). If we focus on the second of them, we can rewrite it in the form

$$(\tilde{f}_{\mathrm{A_d}}(x^*) - f_{\mathrm{B_d}}(y^*))\delta_{\mathrm{d}} = y^* - \tilde{f}_{\mathrm{A_d}}(y^*),$$

which is equivalent to $\delta_{\mathrm{d}} = \delta_{\max_{\mathrm{d}}}$. Hence, if $\delta_{\max_{\mathrm{d}}} \notin \mathring{D}$, then (x^*, y^*) does not satisfy (A.3) for any $\delta_{\mathrm{d}} \in \mathring{D}$. Consequently, H has no stationary points in the interior of its domain and is strictly monotonic in D, which proves the first statement.

Assume now $\delta_{\max_{\mathrm{d}}} \in \mathring{D}$. In that case, (x^*, y^*) satisfies (A.3) only for $\delta_{\mathrm{d}} = \delta_{\max_{\mathrm{d}}}$, and thus H has this point as the only stationary point in the interior of its domain. To study the monotonicity of H on either side of that point, we study the sign of the second derivative of H at it. By differentiating (A.6) with respect to δ_{d} and substituting $\delta_{\mathrm{d}} = \delta_{\max_{\mathrm{d}}}$, we obtain

$$\begin{aligned}(N^*_{\mathrm{A_d}})''(\delta_{\max_{\mathrm{d}}}) + (N^*_{\mathrm{B_d}})''(\delta_{\max_{\mathrm{d}}}) = \\ (N^*_{\mathrm{A_d}})''(\delta_{\max_{\mathrm{d}}}) f'_{\mathrm{A_d}}(x^*) + (N^*_{\mathrm{B_d}})''(\delta_{\max_{\mathrm{d}}}) f'_{\mathrm{B_d}}(y^*) \\ +((N^*_{\mathrm{A_d}})'(\delta_{\max_{\mathrm{d}}}))^2 f''_{\mathrm{A_d}}(x^*) + ((N^*_{\mathrm{B_d}})'(\delta_{\max_{\mathrm{d}}}))^2 f''_{\mathrm{B_d}}(y^*).\end{aligned}$$

We have seen that $f'_{\mathrm{B_d}}(y^*) = f'_{\mathrm{A_d}}(x^*)$ and $(N^*_{\mathrm{B_d}})'(\delta_{\max_{\mathrm{d}}}) = -(N^*_{\mathrm{A_d}})'(\delta_{\max_{\mathrm{d}}})$, and thus

$$(1 - f'_{\mathrm{A_d}}(x^*))H''(\delta_{\max_{\mathrm{d}}}) = ((N^*_{\mathrm{A_d}})'(\delta_{\max_{\mathrm{d}}}))^2 (f''_{\mathrm{A_d}}(x^*) + f''_{\mathrm{B_d}}(y^*)).$$

Since $f''_{\mathrm{A_d}}(x) < 0$ and $f''_{\mathrm{B_d}}(y) < 0$ for all $(x, y) \in \mathbb{R}^2_+$, we have that

$$H''(\delta_{\max_{\mathrm{d}}}) < 0 \iff 1 - f'_{\mathrm{A_d}}(x^*) > 0 \iff x^* > \frac{\tilde{K}_{\mathrm{A_d}}(\sqrt{\tilde{r}_{\mathrm{A_d}}} - 1)}{\tilde{r}_{\mathrm{A_d}} - 1},$$

which is true since $\tilde{K}_{\mathrm{A_d}} < 0$ and $\tilde{r}_{\mathrm{A_d}} < 1$. Therefore, $\delta_{\mathrm{d}} = \delta_{\max_{\mathrm{d}}}$ is a local maximum of H. Since it is the unique stationary point in the interior of its domain, it is the global maximum and, moreover, H is strictly increasing in $[0, \delta_{\max_{\mathrm{d}}})$ and strictly decreasing in $D \setminus [0, \delta_{\max_{\mathrm{d}}})$, which proves the second statement.

□

Figure 3 illustrates the situations described in Proposition 4. Panels (a), (d) and (e) correspond to the first case in Proposition 4, for which the graph is monotonic, either increasing or decreasing. Panels (b) and (c) correspond to the second case, for which the ATPS reaches a maximum at the abscissa $\delta_{\max_{\mathrm{d}}}$.

Appendix B. Continuous time

In the following, we revise system (3.2) of [21] to align it with our system (2) in the effective source–sink case. For consistency, we begin with the original notation from [21]. Their system (3.2) is a source–sink model and reads

$$\begin{aligned}\frac{dN_1}{dt} &= r_1 N_1(1-\frac{N_1}{K_1}) + D(N_2 - sN_1),\\ \frac{dN_2}{dt} &= \bar{r}_2 N_2(-1-\frac{N_2}{K_2}) + D(sN_1 - N_2),\end{aligned}$$

where N_1, N_2 denote the subpopulation sizes, $r_1, \bar{r}_2 > 0$ represent the intrinsic growth rates and $K_1, K_2 > 0$ are the carrying capacities in patches 1 and 2, respectively. Parameter D represents the dispersal rate and s the dispersal asymmetry.
In our work, we use a different notation, but the models correspond to each other as follows. We denote the dispersal rate as $\delta_{\mathrm{c}} = D$ and set s equal to one. Their source population N_1 corresponds to our source population N_{B} in system (2) with $r_1 = r_{\mathrm{B_c}} > 0, K_1 = K_{\mathrm{B_c}} > 0$. Their sink population N_2 corresponds to our effective sink population N_{A} in system (2) with $\bar{r}_2 = |\tilde{r}_{\mathrm{A_c}}|$, $\tilde{r}_{\mathrm{A_c}} < 0$ and $K_2 = |\tilde{K}_{\mathrm{A_c}}|$, $\tilde{K}_{\mathrm{A_c}} < 0$.

Appendix B.1. Stability of equilibria

We rewrite Proposition 5.5 from [21] in our notation to address the stability of the equilibria. We denote $\delta_{\mathrm{crit_c}} = \frac{r_{\mathrm{B}}|\tilde{r}_{\mathrm{A}}|}{|\tilde{r}_{\mathrm{A}}|-r_{\mathrm{B}}}$, $\mathbb{R}^2_+ := [0,+\infty)\times[0,+\infty)$ and $\mathbb{R}^2_{++} := (0,+\infty)\times(0,+\infty)$.

Proposition 5.5 [21]. Let $\delta_{\mathrm{c}} > 0$.

(i) Assume $|\tilde{r}_{\mathrm{A_c}}| \le r_{\mathrm{B_c}}$, or $|\tilde{r}_{\mathrm{A_c}}| > r_{\mathrm{B_c}}, \delta_{\mathrm{c}} < \delta_{\mathrm{crit_c}}$. System (2) has a unique positive equilibrium $(N^*_{\mathrm{A}}, N^*_{\mathrm{B}})$, which is globally asymptotically stable in $\mathbb{R}^2_{++}$.

(ii) Assume $|\tilde{r}_{\mathrm{A_c}}| > r_{\mathrm{B_c}}$ and $\delta_{\mathrm{c}} \geq \delta_{\mathrm{crit_c}}$. System (2) has no positive equilibrium, and the extinction equilibrium $(N_{\mathrm{A}}^*, N_{\mathrm{B}}^*) = (0, 0)$ is globally asymptotically stable in $\mathbb{R}_+^2$.

Appendix B.2. Response scenarios

Proposition 5.11 in [21] categorises five cases how increasing dispersal affects the ATPS in the presence of asymmetric dispersal. We rewrite the proposition using our notation and align their cases with our response scenarios, adding comments on each of the cases in italic. Cases (ii) and (iii) are not attainable in our model with symmetric dispersal, and thus we have excluded them. Denote the ATPS at perfect mixing as ATPS_∞, at zero dispersal as ATPS_0 and between isolation and perfect mixing as $\mathrm{ATPS}_{\mathrm{c}}$.

Proposition 5.11 [21]. Assume $\delta_{\mathrm{c}} > 0$.

(i) Let $|\tilde{r}_{\mathrm{A_c}}| > r_{\mathrm{B_c}}$. Then $\mathrm{ATPS}_{\mathrm{c}} < \mathrm{ATPS}_0$. If $\delta_{\mathrm{c}} < \delta_{\mathrm{crit_c}}$, then $\mathrm{ATPS}_\infty > 0$. If $\delta_{\mathrm{c}} \geq \delta_{\mathrm{crit_c}}$, then $\mathrm{ATPS}_\infty = 0$.
This case corresponds to the extinction response scenario (see Fig. 3(e)).

(iv) Let $r_{\mathrm{B_c}} > |\tilde{r}_{\mathrm{A_c}}|$, $\frac{\tilde{K}_{\mathrm{A_c}}(r_{\mathrm{B_c}} - |\tilde{r}_{\mathrm{A_c}}|)}{|\tilde{r}_{\mathrm{A_c}}|(\tilde{K}_{\mathrm{A_c}} + K_{\mathrm{B_c}})} < 1$. There is $\delta_{\mathrm{c}}^\dagger > 0$ such that $\mathrm{ATPS}_{\mathrm{c}} > \mathrm{ATPS}_0$ as $\delta_{\mathrm{c}} < \delta_{\mathrm{c}}^\dagger$, while $\mathrm{ATPS}_{\mathrm{c}} < \mathrm{ATPS}_0$ as $\delta_{\mathrm{c}} < \delta_{\mathrm{c}}^\dagger$ with $\mathrm{ATPS}_\infty > 0$.
This case corresponds to the beneficial turning detrimental response scenario (see Fig. 3(c)).

(v) Let $r_{\mathrm{B_c}} > |\tilde{r}_{\mathrm{A_c}}|$, $\frac{\tilde{K}_{\mathrm{A_c}}(r_{\mathrm{B_c}} - |\tilde{r}_{\mathrm{A_c}}|)}{|\tilde{r}_{\mathrm{A_c}}|(\tilde{K}_{\mathrm{A_c}} + K_{\mathrm{B_c}})} \geq 1$. Then, $\mathrm{ATPS}_{\mathrm{c}} > \mathrm{ATPS}_0$. Moreover, $\mathrm{ATPS}_\infty > \mathrm{ATPS}_0$ as $\frac{\tilde{K}_{\mathrm{A_c}}(r_{\mathrm{B_c}} - |\tilde{r}_{\mathrm{A_c}}|)}{|\tilde{r}_{\mathrm{A_c}}|(\tilde{K}_{\mathrm{A_c}} + K_{\mathrm{B_c}})} > 1$, $\mathrm{ATPS}_\infty = \mathrm{ATPS}_0$ as $\frac{\tilde{K}_{\mathrm{A_c}}(r_{\mathrm{B_c}} - |\tilde{r}_{\mathrm{A_c}}|)}{|\tilde{r}_{\mathrm{A_c}}|(\tilde{K}_{\mathrm{A_c}} + K_{\mathrm{B_c}})} = 1$.
This case corresponds to both the unimodally beneficial and monotonically beneficial response scenarios (see Fig. 3(a,b)).

References

[1] IPBES, Summary for policymakers of the thematic assessment of the sustainable use of wild species of the Intergovernmental Science-Policy Platform on Biodiversity and Ecosystem Services, *https://zenodo.org/record/6425599*, Bonn, Germany, 2022. doi:10.5281/ZENODO.6425599.

[2] D. T. Bolger, W. D. Newmark, T. A. Morrison, D. F. Doak, The need for integrative approaches to understand and conserve migratory ungulates, Ecology Letters 11 (1) (2007) 63–77. doi:10.1111/j.1461-0248.2007.01109.x.

[3] E. A. Fulton, N. J. Bax, R. H. Bustamante, J. M. Dambacher, C. Dichmont, P. K. Dunstan, K. R. Hayes, A. J. Hobday, R. Pitcher, E. E. Plagányi, A. E. Punt, M. Savina-Rolland, A. D. M. Smith, D. C. Smith, Modelling marine protected areas: insights and hurdles, Philosophical Transactions of the Royal Society B: Biological Sciences 370 (1681) (2015) 20140278. doi:10.1098/rstb.2014.0278.
URL `http://dx.doi.org/10.1098/rstb.2014.0278`

[4] E. Sala, S. Giakoumi, No-take marine reserves are the most effective protected areas in the ocean, ICES Journal of Marine Science 75 (3) (2017) 1166–1168. doi:10.1093/icesjms/fsx059.

[5] R. Goñi, R. Hilborn, D. Díaz, S. Mallol, S. Adlerstein, Net contribution of spillover from a marine reserve to fishery catches, Marine Ecology Progress Series 400 (2010) 233–243. doi:10.3354/meps08419.

[6] H. S. Robinson, R. Desimone, C. Hartway, J. A. Gude, M. J. Thompson, M. S. Mitchell, M. Hebblewhite, A test of the compensatory mortality hypothesis in mountain lions: A management experiment in west-central Montana, The Journal of Wildlife Management 78 (5) (2014) 791–807. doi:10.1002/jwmg.726.

[7] COP15, Conference of the parties to the convention on biological diversity. Fifteenth meeting - part II, *https://www.cbd.int/meetings/COP-15*, Montreal, Canada, 2023.

[8] D. L. DeAngelis, D. Franco, A. Hastings, F. M. Hilker, S. Lenhart, F. Lutscher, N. Petrovskaya, S. Petrovskii, R. C. Tyson, Towards building a sustainable future: positioning ecological modelling for impact in ecosystems management, Bulletin of Mathematical Biology 83 (10) (2021) 1–28. doi:10.1007/s11538-021-00927-y.

[9] J. C. Pezzey, C. M. Roberts, B. T. Urdal, A simple bioeconomic model of a marine reserve, Ecological Economics 33 (1) (2000) 77–91. doi:10.1016/s0921-8009(99)00129-9.

[10] M. G. Neubert, Marine reserves and optimal harvesting, Ecology Letters 6 (9) (2003) 843–849. doi:10.1046/j.1461-0248.2003.00493.x.

[11] E. González-Olivares, J. Huincahue-Arcos, A two-patch model for the optimal management of a fishing resource considering a marine protected area, Nonlinear Analysis: Real World Applications 12 (5) (2011) 2489–2499. doi:10.1016/j.nonrwa.2011.02.012.

[12] H. V. Moeller, M. G. Neubert, Economically optimal marine reserves without spatial heterogenity in a simple two-patch model, Natural Resource Modeling 28 (3) (2015) 244–255. doi:10.1111/nrm.12066.

[13] P. Lundberg, N. Jonzén, Spatial population dynamics and the design of marine reserves, Ecology Letters 2 (3) (1999) 129–134. doi:10.1046/j.1461-0248.1999.00064.x.

[14] H. R. Pulliam, Sources, sinks, and population regulation, The American Naturalist 132 (5) (1988) 652–661. doi:10.1086/284880.

[15] A. T. H. Keeley, P. Beier, T. Creech, K. Jones, R. H. Jongman, G. Stonecipher, G. M. Tabor, Thirty years of connectivity conservation planning: an assessment of factors influencing plan implementation, Environmental Research Letters 14 (10) (2019) 103001. doi:10.1088/1748-9326/ab3234.

[16] L. W. Botsford, A. Hastings, Conservation dynamics of marine metapopulations with dispersing larvae, in: Marine Metapopulations, J. P. Kritzer and P. F. Sale (Eds.), Academic Press, New York, 2006, Ch. 12, p. 411–429. doi:10.1016/b978-012088781-1/50015-7.

[17] A. Hastings, L. W. Botsford, Equivalence in yield from marine reserves and traditional fisheries management, Science 284 (5419) (1999) 1537–1538. doi:10.1126/science.284.5419.1537.

[18] D. R. Lockwood, A. Hastings, L. W. Botsford, The effects of dispersal patterns on marine reserves: Does the tail wag the dog?, Theoretical Population Biology 61 (3) (2002) 297–309. doi:10.1006/tpbi.2002.1572.

[19] R. Arditi, C. Lobry, T. Sari, Is dispersal always beneficial to carrying capacity? New insights from the multi-patch logistic equation, Theoretical Population Biology 106 (2015) 45–59. doi:10.1016/j.tpb.2015.10.001.

[20] D. Gao, Y. Lou, Total biomass of a single population in two-patch environments, Theoretical Population Biology 146 (2022) 1–14. doi:10.1016/j.tpb.2022.05.003.

[21] H. Wu, Y. Wang, Y. Li, D. L. DeAngelis, Dispersal asymmetry in a two-patch system with source–sink populations, Theoretical Population Biology 131 (2020) 54–65. doi:10.1016/j.tpb.2019.11.004.

[22] C. Grumbach, F. N. Reurik, J. Segura, D. Franco, F. M. Hilker, The effect of dispersal on asymptotic total population size in discrete- and continuous-time two-patch models, Journal of Mathematical Biology 87 (4) (2023) 60. doi:10.1007/s00285-023-01984-8.

[23] A. R. Ives, S. T. Woody, E. V. Nordheim, C. Nelson, J. H. Andrews, The synergistic effects of stochasticity and dispersal on population densities, The American Naturalist 163 (3) (2004) 375–387. doi:10.1086/381942.

[24] B. Zhang, A. Kula, K. M. L. Mack, L. Zhai, A. L. Ryce, W. Ni, D. L. DeAngelis, J. D. Van Dyken, Carrying capacity in a heterogeneous environment with habitat connectivity, Ecology Letters 20 (9) (2017) 1118–1128. doi:10.1111/ele.12807.

[25] I. Vortkamp, C. Kost, M. Hermann, F. M. Hilker, Dispersal between interconnected patches can reduce the total population size, bioRxiv 2022.04.28.489935 (2022). doi:10.1101/2022.04.28.489935.

[26] S. Dey, B. Goswami, A. Joshi, Effects of symmetric and asymmetric dispersal on the dynamics of heterogeneous metapopulations: two-patch systems revisited, Journal of Theoretical Biology 345 (2014) 52–60. doi:10.1016/j.jtbi.2013.12.005.

[27] R. D. Holt, Population dynamics in two-patch environments: Some anomalous consequences of an optimal habitat distribution, Theoretical Population Biology 28 (2) (1985) 181–208. doi:10.1016/0040-5809(85)90027-9.

[28] D. Franco, A. Ruiz-Herrera, To connect or not to connect isolated patches, Journal of Theoretical Biology 370 (2015) 72–80. doi:10.1016/j.jtbi.2015.01.029.

[29] R. M. Sibly, D. Barker, M. C. Denham, J. Hone, M. Pagel, On the regulation of populations of mammals, birds, fish, and insects, Science 309 (5734) (2005) 607–610. doi:10.1126/science.1110760.

[30] R. Bravo de la Parra, J.-C. Poggiale, P. Auger, The effect of connecting sites in the environment of a harvested population, Mathematical Modelling of Natural Phenomena 18 (4) (2023). doi:10.1051/mmnp/2023004.

[31] G. N. Tuck, H. P. Possingham, Optimal harvesting strategies for a metapopulation, Bulletin of Mathematical Biology 56 (1) (1994) 107–127. doi:10.1007/bf02458291.

[32] J. N. Sanchirico, J. E. Wilen, A bioeconomic model of marine reserve creation, Journal of Environmental Economics and Management 42 (3) (2001) 257–276. doi:10.1006/jeem.2000.1162.

[33] G. J. Edgar, R. D. Stuart-Smith, T. J. Willis, S. Kininmonth, S. C. Baker, S. Banks, N. S. Barrett, M. A. Becerro, A. T. F. Bernard, J. Berkhout, C. D. Buxton, S. J. Campbell, A. T. Cooper, M. Davey, S. C. Edgar, G. Försterra, D. E. Galván, A. J. Irigoyen, D. J. Kushner, R. Moura, P. E. Parnell, N. T. Shears, G. Soler, E. M. A. Strain, R. J. Thomson, Global conservation outcomes depend on marine protected areas with five key features, Nature 506 (7487) (2014) 216–220. doi:10.1038/nature13022.

[34] J. Geldmann, L. Coad, M. D. Barnes, I. D. Craigie, S. Woodley, A. Balmford, T. M. Brooks, M. Hockings, K. Knights, M. B. Mascia, L. McRae, N. D. Burgess, A global analysis of management capacity and ecological outcomes in terrestrial protected areas, Conservation Letters 11 (3) (2018) e12434. doi:10.1111/conl.12434.

[35] S. Kirkland, C.-K. Li, S. J. Schreiber, On the evolution of dispersal in patchy landscapes, SIAM Journal on Applied Mathematics 66 (4) (2006) 1366–1382. doi:10.1137/050628933.